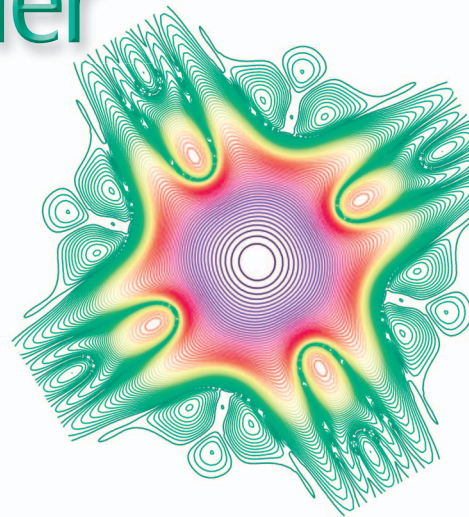


# OFDM Versus Filter Bank Multicarrier

[Development of broadband communication systems]

[Behrouz Farhang-Boroujeny]



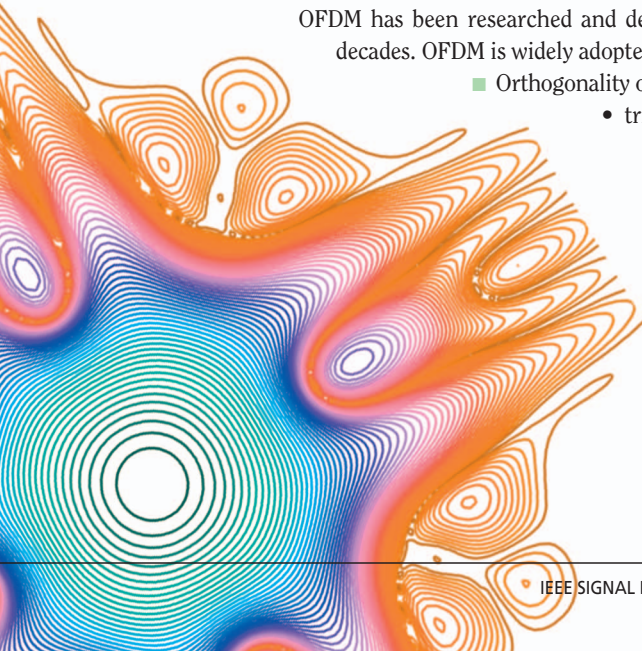
**A**s of today, orthogonal frequency division multiplexing (OFDM) has been the dominant technology for broadband multicarrier communications. However, in certain applications such as cognitive radios and uplink of multiuser multicarrier systems, where a subset of subcarriers is allocated to each user, OFDM may be an undesirable solution. In this article, we address the shortcomings of OFDM in these and other applications and show that filter bank multicarrier (FBMC) could be a more effective solution. Although FBMC methods have been studied by a number of researchers, and some even before the invention of OFDM, only recently has FBMC been seriously considered by a few standard committees. The goal of this article is to bring this upcoming trend to the attention of the signal processing and communications communities and to motivate more research in this important area.

## INTRODUCTION

OFDM has been researched and deployed for broadband wired and wireless communications for the past two decades. OFDM is widely adopted because of a number of advantages that it offers:

- Orthogonality of subcarrier signals that allows
  - trivial generation of transmit signal through an inverse fast Fourier transform (IFFT) block
  - trivial separation of the transmitted data symbols at the receiver through a fast Fourier transform (FFT) block
    - trivial equalization through a scalar gain per subcarrier
    - trivial adoption to multiple-input multiple-output (MIMO) channels.
- Closely spaced orthogonal subcarriers partition the available bandwidth into a maximum collection of narrow subbands.
- Adaptive modulation schemes can be applied to subcarrier bands to maximize bandwidth efficiency/transmission rate.

*Digital Object Identifier 10.1109/MSP.2011.940267*  
*Date of publication: 19 April 2011*



■ The very special structure of OFDM symbols simplifies the tasks of carrier and symbol synchronizations.

These points are well understood and documented in the literature [1], [2]. On the other hand, multiple-access OFDM or orthogonal frequency division multiple access (OFDMA) has been recently proposed in a number of standards and proprietary waveforms (e.g., [3]). Some particular forms of OFDMA have also been proposed for cognitive radio systems [5]. In OFDMA, each user is allocated a subset of subcarriers. To prevent intercarrier interference (ICI), the users' signals must be synchronized at the receiver input (but not necessarily at the transmitters' outputs). Considering this point, one may note that OFDMA only works well in the network downlink of a base station, where all of the subcarriers are transmitted from the same point (the base station) and hence can be easily synchronized and undergo the same Doppler frequency shift before reaching each receiver. However, synchronization is not trivial in the uplink where a number of nodes are transmitting separately. Since, in practice, perfect synchronization in the uplink of an OFDMA network may not be possible, additional signal-processing steps have to be taken to minimize interference among signals from different nodes. Such steps add significant complexity to an OFDMA receiver; see [4] and the references therein.

The problem is worse in a cognitive radio setting where both primary (noncognitive nodes) and secondary users (cognitive nodes) transmit independently and may be based on different standards. In such a setting, the only way that one may adopt to separate the primary and secondary user signals is through a filtering mechanism. OFDM is thus a poor fit because the filters associated with its synthesized subcarrier signals (at the transmitter) and analyzed subcarrier signals (at the receiver) have relatively large side lobes and such lobes will result in leakage of signal powers among the bands of different users [7]. Although suggestions have been made to improve the side lobes of OFDM analysis and synthesis filters through the use of filtered OFDM [5] (discussed later) and other methods [6], these solutions are generally very limited in performance.

Furthermore, data transmissions over digital subscriber lines (DSLs) and power line communication (PLC) technologies often use unshielded wires and thus become a source and victim of electromagnetic interference. This is similar to the case of OFDMA and cognitive radios, where each transmission can be established over certain portions of a broadband, and spectral activities over the rest of the band should be avoided to allow coexistence with radio communication activities within the band of interest.

The above problems could be greatly alleviated if the filters that synthesize/analyze the subcarrier signals had small side lobes. An interesting, but apparently not widely understood, fact is that the first multicarrier technique developed before the invention of OFDM [10] used filter banks for the synthesis and analysis of multicarrier signals. Such filter banks can be designed with arbitrarily small side lobes and, therefore, are an ideal choice in multiple access and cognitive radio applications as well as broadband data transmission over unshielded wires.

The goal of this article is to present a tutorial review of FBMC techniques and compare them with OFDM in various applications. We note that most of the advantages of FBMC originate from the fact that, by design, the nonadjacent subcarriers in this modulation are separated almost perfectly through a bank of well-designed filters. OFDM, on the other hand, was originally designed with a great emphasis on a low-complexity implementation. Much of the low complexity of OFDM is due to a fundamental assumption: subcarrier signals are a set of perfectly synchronized orthogonal tones. These tones are generated at the transmitter using an IFFT block, and they are separated at the receiver through an FFT block.

Although this article highlights a number of limitations of OFDM in present and future communication systems, the author has no intention of ignoring the many important and desirable features of OFDM that were itemized at the beginning of this section. The intention is to emphasize the fact that OFDM, although widely adopted in the present industry, is not necessarily the best solution in many future communication systems, particularly in multiple access and cognitive radio networks where FBMC may be found more appealing. At the same time, the limitations of FBMC will be noted. For instance, we note that while deployment of a MIMO technique in OFDM is a straightforward task, unfortunately, the development of MIMO-FBMC systems/networks is nontrivial and may be very limited. Moreover, while for many applications, FBMC may be more complex than OFDM, there are cases where the added steps to undo the undesirable features of OFDM may lead to systems that are more complex than their FBMC counterparts.

This article is organized as follows. To draw a connection between OFDM and FBMC, a unified filter bank formulation that is applicable to both is presented in the section "A Unified Formulation for OFDM and FBMC." This formulation shows that the prototype filter based on which an OFDM signal is synthesized/analyzed has to obey certain constraints, and it is these constraints that result in the undesirable performance of OFDM in the applications discussed in [7] and those that we further discuss in this article. Filtered OFDM, a modified OFDM that has been designed to improve on the spectral containment of subcarrier signals, is then presented and discussed in detail in the section "Filtered OFDM." This presentation shows some of the serious limitations of a filtered OFDM in restricting the spectra of desired subcarriers to any band of interest. FBMC systems are reviewed in the section "Filter Bank Multicarrier." This presentation is structured to clearly show the spectral advantages of FBMC over OFDM. The applications of multicarrier techniques are reviewed in the section "Applications." This section is organized to highlight the pros and cons of both OFDM and FBMC systems in a variety of current and future applications. To present the basic ideas behind OFDM and FBMC methods, without getting too far into the details, the presentations in sections "A Unified Formulation for OFDM and FBMC," "Filtered OFDM," and "Filter Bank Multicarrier" ignore some parts of the literature. This

compromise is made to keep the intended tutorial feature of the article. To fill this gap, the section “Additional Notes” provides a brief overview of some important recent developments in the area of FBMC. The section “Conclusions” presents the concluding remarks of this article.

## A UNIFIED FORMULATION FOR OFDM AND FBMC

Figure 1 presents a block diagram that is commonly used to depict an FBMC transceiver. This structure is also applicable to OFDM. We note that although, in practice, the synthesis and analysis filter banks are implemented in discrete time, we have chosen to present them in terms of continuous time filters, as this formulation serves our discussion the best.

The inputs in Figure 1 are the data signals defined as

$$s_k(t) = \sum_n s_k[n] \delta(t - nT), \quad (1)$$

where  $s_k[n]$ s are the subcarrier data symbols,  $k$  is a subcarrier index, and  $T$  is the symbol time spacing.

The difference between OFDM and FBMC lies in the choice of  $T$  and the transmitter and receiver prototype filters  $p_T(t)$  and  $p_R(t)$ , respectively. In a conventional OFDM,  $p_T(t)$  is a rectangular pulse of height one and width  $T$ . The receiver prototype filter  $p_R(t)$  is also a rectangular pulse of height one, but its width is reduced to  $T_{\text{FFT}} < T$ , where  $T_{\text{FFT}} = 1/B$ , and  $B$  is the frequency spacing between subcarriers. (We note that the notation  $T_{\text{FFT}}$  is used here since this is equal to the time duration over which the received signal is sampled and passed through an FFT block [1], [2].) In FBMC systems that are designed for maximum bandwidth efficiency,  $T = T_{\text{FFT}} = 1/B$ , however, the durations of  $p_T(t)$  and  $p_R(t)$  are greater than  $T$  (usually, an integer multiple of  $T$ ). Hence, in FBMC, the successive data symbols overlap.

The use of prototype filters with rectangular impulse responses leads to undesirable magnitude responses that suffer from large side lobes in the frequency domain. This follows immediately from the fact that the Fourier transform of a rectangular pulse is a sinc function, and it is well known that the side lobes of a sinc pulse are relatively large; the peak of the first side lobe is only 13 dB below the peak of its main lobe. To combat this problem, in some standards, e.g., in very-high-bit rate DSL (VDSL) [22], [23] and PLCs [48], [49],

the rectangular pulse shape, with sharp edges, is replaced by a pulse shape with smooth edges; see also [24]–[27]. In this article, we use the term filtered OFDM to refer to the cases where the rectangular window is replaced by a window with smooth edges.

## FILTERED OFDM

### FUNDAMENTAL CONCEPTS

From the structure depicted in Figure 1, the transmit signal is obtained as

$$x(t) = \sum_n \sum_{k \in \mathcal{K}} s_k[n] p_T(t - nT) e^{j2\pi n T f_k}, \quad (2)$$

where  $\mathcal{K}$  denotes a set of active symbol indices and  $j = \sqrt{-1}$ . In a conventional OFDM where  $p_T(t)$  is a rectangular pulse, (2) may be read as follows. For every  $n$ ,  $x(t)$  is generated by adding a number of time-limited complex-valued tones, whose magnitude and phase are determined by the data symbols  $s_k[n]$ s. These tones, when passed through the channel, after the transient period of the channel response, will be the same tones modified by the channel gains at the respective frequencies.

Separating different subcarriers, (2) can be written as

$$x(t) = \sum_{k \in \mathcal{K}} x_k(t), \quad (3)$$

where

$$x_k(t) = \sum_n s_k[n] p_{T,k}(t - nT) \quad (4)$$

and

$$p_{T,k}(t) = p_T(t) e^{j2\pi t f_k}. \quad (5)$$

We note that (4) may be viewed as a filtering operation applied to a sequence of impulses, modulated by the data symbols  $s_k[n]$ s. The filter  $p_{T,k}(t)$  is obtained by modulating the prototype filter  $p_T(t)$ .

Alternatively, (2) may be written as

$$x(t) = \sum_n \sum_{k \in \mathcal{K}} s_k[n] p_{T,k}(t - nT). \quad (6)$$

Assuming an ideal channel, the received signal  $y(t)$  is the same as the transmit signal  $x(t)$ . In that case, the data symbols  $s_k[n]$ , for  $k \in \mathcal{K}$ , and all values of  $n$  will be separable if

$$\langle p_{T,k}(t - mT), p_{R,l}(t - nT) \rangle = \delta_{kl} \delta_{nm}, \quad (7)$$

where

$$\langle p_{T,k}(t - mT), p_{R,l}(t - nT) \rangle = \int_{-\infty}^{\infty} p_{T,k}(t - mT) p_{R,l}^*(t - nT) dt, \quad (8)$$

\* denotes a complex conjugate, and  $\delta_{kl}$  is the Kronecker delta function defined as

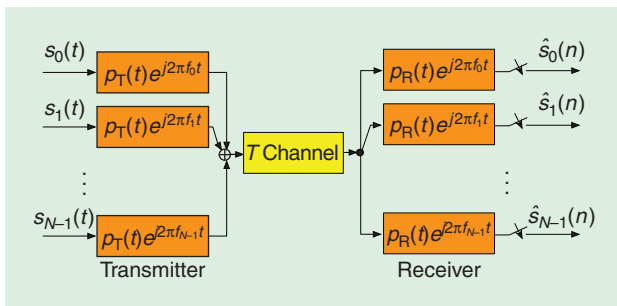


**[FIG1]** Block diagram of an FBMC transceiver. This structure is also applicable to OFDM.



$$\delta_{kl} = \begin{cases} 1, & k = l, \\ 0, & k \neq l. \end{cases} \quad (9)$$

We note that (8) is the inner product of two signals/functions. Also, for obvious reasons, we refer to (7) as the orthogonality condition.

To satisfy the orthogonality condition (7), OFDM modulation and demodulation have been developed based on the following result. The time-limited complex-valued tones

$$a_k(t) = \begin{cases} e^{j\frac{2\pi}{\tau}kt}, & 0 \leq t < \tau, \\ 0, & \text{otherwise} \end{cases} \quad (10)$$

for all integer values of  $k$  are a set of orthogonal functions. Using this result, one will find that the orthogonality condition (7) holds if  $p_T(t)$  is a rectangular pulse of width  $T \geq \tau$ ,  $p_R(t)$  is a rectangular pulse of width  $\tau$ , and the subcarriers are spaced at the regular frequency spacing  $1/\tau$ . In OFDM,  $\tau = T_{\text{FFT}}$ .

In the absence of a channel, a trivial choice of  $p_T(t)$  and  $p_R(t)$  is a pair of rectangular pulses with equal duration  $\tau$ . In the presence of a channel, each transmitted tone will undergo a transient before reaching a steady state. To accommodate the transient period, the duration of  $p_T(t)$  is extended by an interval greater than the duration of the channel impulse response, and at the receiver,  $p_R(t)$  is time aligned with the transmitted tone after it has reached steady state. This is illustrated in Figure 2. The duration of  $p_T(t)$  is extended by the process of adding a cyclic prefix (CP) to each OFDM symbol. This is elaborated further below.

In a practical implementation of an OFDM system, modulation and demodulation are performed digitally using an IFFT and an FFT, respectively. The width of  $p_R(t)$ ,  $\tau$ , is set equal to  $T_{\text{FFT}} = NT_s$ , where  $T_s$  is the time space between samples at the IFFT output and FFT input, and  $N$  is the length of the FFT and IFFT blocks. Accordingly, the carrier tones are generated at the normalized frequencies  $f = 0, 1/N, 2/N, \dots, (N-1)/N$ . Clearly, the width of  $p_T(t)$  is set equal to some value  $T > T_{\text{FFT}}$  to accommodate the channel transient period, as in Figure 2. Moreover, one may think of  $T - T_{\text{FFT}}$  as a bandwidth loss that OFDM should suffer to restore the orthogonality of the transmitted tones (respectively, the modulated data symbols) at the receiver.

One instructive tool that will be found useful later, as we explore the bandwidth efficiency of FBMC systems and compare them with OFDM transmission, is the so-called time–frequency phase-space lattice representation. Figure 3 presents the time–frequency phase-space lattice associated with an OFDM system. Each dot indicates a data symbol. The data symbols are transmitted every  $T$  seconds and also spread along the frequency axis at the spacing  $F = 1/T_{\text{FFT}}$ . There is one symbol in each rectangle of area  $T \times F = T/T_{\text{FFT}}$ . Hence, the data symbol density is

$$\frac{1}{TF} = \frac{T_{\text{FFT}}}{T} \leq 1. \quad (11)$$

The upper limit 1 in (11) can only be achieved in an ideal channel, i.e., a channel with a transient period of zero. This is, of

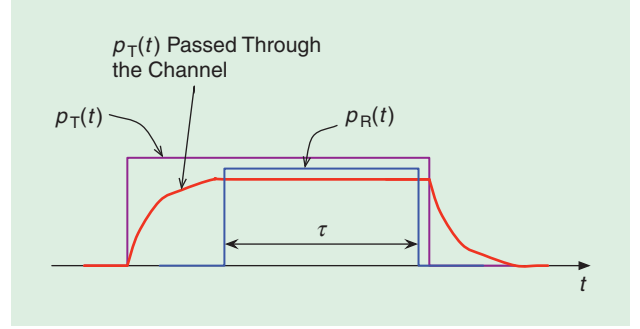


**[FIG2]** An illustration of how orthogonality is established in OFDM.

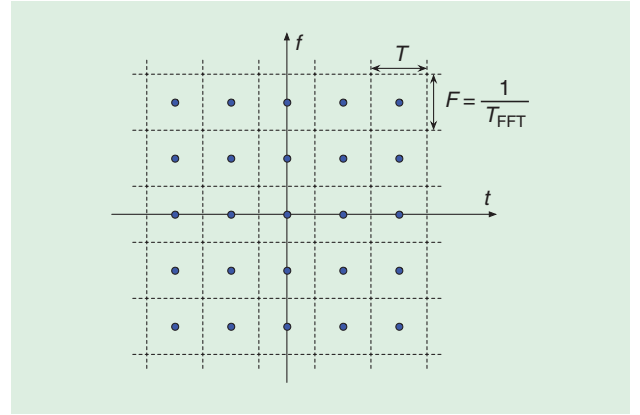


**[FIG3]** Time–frequency phase-space lattice representation of an OFDM system.

course, unrealistic and unachievable in practice. Therefore, it is fair to say that OFDM can only achieve a symbol density of less than one, and the symbol density one can only be thought as an unachievable upper limit.

### FILTERING

In filtered OFDM, the rectangular pulse  $p_T(t)$  that was introduced above is replaced by a pulse (or a window function) that has soft transitions at the beginning and end. The common form of  $p_T(t)$  that is often used in practice is the raised-cosine pulse that is presented in Figure 4(a).  $T_0$  is the period of overlap among each pair of adjacent OFDM symbols and is often referred to as the roll-off period. One may also note that

$$p_T(t) = \Pi\left(\frac{t - T/2}{T}\right) \star h(t), \quad (12)$$

where  $\star$  denotes convolution,

$$\Pi\left(\frac{t}{T}\right) = \begin{cases} 1, & |t| \leq T/2, \\ 0, & \text{otherwise} \end{cases} \quad (13)$$

and

$$h(t) = \frac{\pi}{2T_0} \sin\left(\frac{\pi t}{T_0}\right) \Pi\left(\frac{t - T_0/2}{T_0}\right). \quad (14)$$

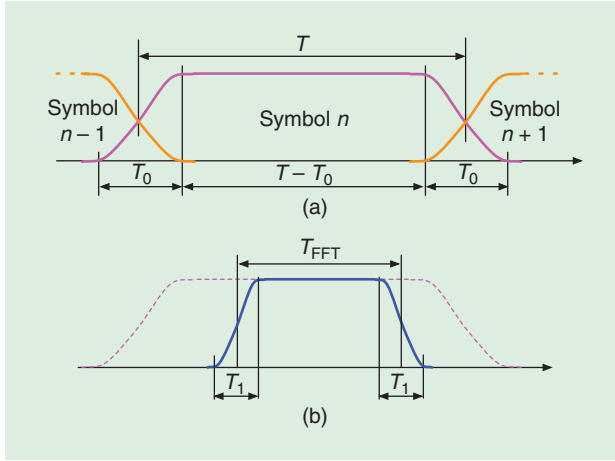


**[FIG4]** Details of the prototype filters in a filtered-OFDM system. (a) Transmitter. (b) Receiver.

This shows that  $p_T(t)$  is obtained by convolving a rectangular pulse of width  $T$  and a half-sine wave of width  $T_0$ . Accordingly, one finds that

$$|P_T(f)| = T|\text{sinc}(fT)| \times |H(f)| \quad (15)$$

and

$$|H(f)| = \left| \frac{\cos(\pi f T_0)}{1 - 4f^2 T_0^2} \right|. \quad (16)$$

Figure 5 presents a set of sample plots of (a)  $|\text{sinc}(fT)|$ , (b)  $|H(f)|$ , and (c)  $(1/T)|P_T(f)| = |\text{sinc}(fT)| \times |H(f)|$ . These plots clearly show that  $P_T(f)$  is a low-pass filter characterized by a narrow-band main lobe, a number of significant side lobes that expand over a bandwidth of  $3/T_0$ , and a number of well-attenuated side lobes at higher frequencies. If one defines the stopband of this filter over the frequencies where  $(1/T)|P_T(f)|$  is  $-50$  dB or less, its transition band has a width of approximately  $3/T_0$ .

In Figure 5(a), it is indicated that the width of the main lobe of  $\text{sinc}(fT)$  is approximately equal to  $2/T_{\text{FFT}}$ . We take this approximation that will become exact when  $T = T_{\text{FFT}}$  to be a desired width of each subcarrier (including both its pass and transition bands). On the other hand, from the above results we may observe that, when the roll-off period  $T_0$  is small, the presence of the large side lobes over a width of  $3/T_0$  significantly violates this desirable goal. In other words, to achieve this goal,  $T_0$  should be comparable with  $T_{\text{FFT}}$ .

Similarly, one may note that the subcarrier filters implemented at the receiver of a filtered-OFDM system will suffer from a wide transition band unless the roll-off period  $T_1$  in Figure 4(b) is made sufficiently wide. On the other hand, by direct inspection of Figure 4(a) and (b), one may note that the following condition should hold:  $T - T_0 > T_{\text{FFT}} + T_1$  or, equivalently,  $T > T_{\text{FFT}} + T_0 + T_1$ . Also, recalling the fundamental concept behind the OFDM operation, one may note that the difference  $T - (T_{\text{FFT}} + T_0 + T_1)$  is a residual time that is allocated to accommodate the duration of the channel impulse

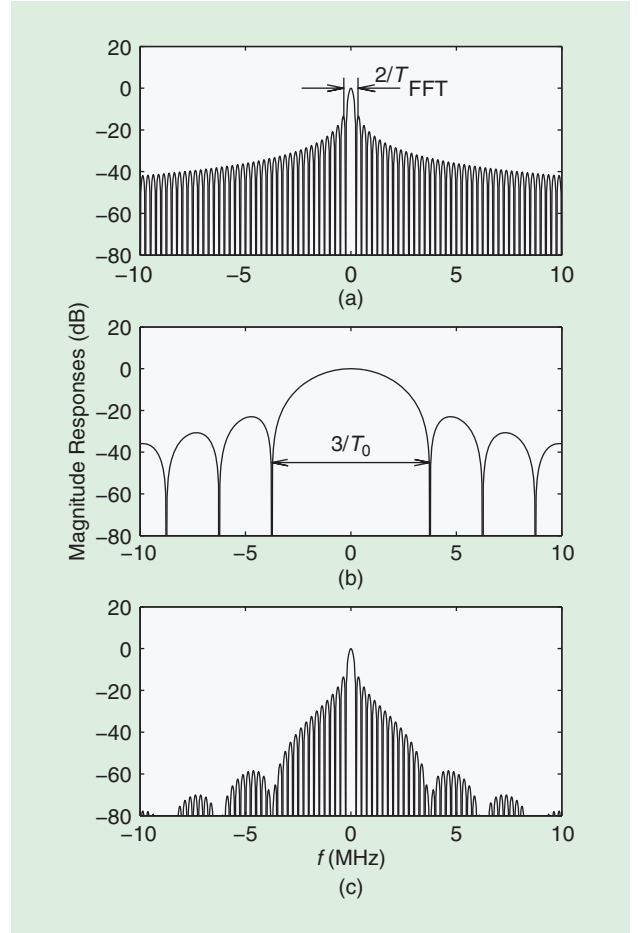


**[FIG5]** Magnitude responses of (a)  $\text{sinc}(fT)$ , (b)  $H(f)$ , and (c)  $\text{sinc}(fT) \times H(f)$ , for  $T = 4 \mu\text{s}$ ,  $T_{\text{FFT}} = 3 \mu\text{s}$ , and  $T_0 = 0.17$ .

response [1], [2]. Recall that this is equivalent to a CP period when  $T_0 = T_1 = 0$ .

#### BANDWIDTH EFFICIENCY

We note that, in (filtered) OFDM, each set of data symbols  $s_k[n]$ , for  $k \in \mathcal{K}$  and a fixed value of  $n$ , is transmitted over a time period of  $T$  seconds. From this, only  $T_{\text{FFT}}$  seconds is allocated to a nonredundant signal. The rest of the time period  $T$  is allocated to the transmission of CP (and possibly suffix) signals that may be referred to as overhead. We note that this overhead is necessary to allow the transmitter and receiver filtering operations that were discussed above as well as to take care of the transition period introduced by the channel impulse response. We thus define the bandwidth efficiency of OFDM by the parameter

$$\eta = \frac{T_{\text{FFT}}}{T} \times 100\% \quad (17)$$

and note that  $T = T_{\text{FFT}} + T_0 + T_1 + T_{\text{ch}}$ , where  $T_0$  and  $T_1$  are the time periods defined in Figure 4 and  $T_{\text{ch}}$  is the maximum time allowed for the duration of the channel impulse response.

Clearly, to maximize the bandwidth efficiency of OFDM, one should choose the time periods  $T_0$ ,  $T_1$ , and  $T_{\text{ch}}$  as small as possible. However, the size of  $T_{\text{ch}}$  is dictated by the channel characteristics, and  $T_0$  and  $T_1$  should be chosen according to some desired filtering targets. In particular, in a multiuser application, to allow different users in the channels in close proximity to one another,  $T_0$  and  $T_1$  should be given large values (comparable to  $T_{\text{FFT}}$ ). Clearly, such choices will be counterproductive as they result in a different form of bandwidth loss through the parameter  $\eta$ . Hence, in any case, OFDMA suffers from a significant spectral inefficiency unless near-perfect synchronization could be achieved and/or the advanced (and complex) processing steps discussed in [4] are applied. Further discussions on the filtering limitation in filtered OFDM and its optimization are presented in “Filtered OFDM: Limitations and Optimizations.”

### FILTER BANK MULTICARRIER

In FBMC, a set of parallel data symbols  $s_k[n]$  are transmitted through a bank of modulated filters, as in Figure 1, and, thus, the transmit signal is synthesized according to (2). The difference between OFDM and FBMC lies in the choice of the prototype filters  $p_T(t)$  and  $p_R(t)$ . Also, the selection of  $p_T(t)$  and  $p_R(t)$  varies depending on the adopted FBMC modulation technique. Here, we present FBMC systems under two distinct classes. The first class of FBMC systems that we introduce are designed to transmit complex-valued [i.e., quadrature amplitude-modulated (QAM)] data symbols. The second class of FBMC systems that will be presented are limited to transmission of real-valued [i.e., pulse amplitude-modulated (PAM)] data symbols. Both methods (FBMC classes) have their roots in early developments of digital data communication systems. They were originally developed in the 1960s, prior to the development of OFDM systems. Moreover, a number of recent developments have made them very attractive for making efficient use of broadband spectra both in doubly dispersive channels (defined below) and in multiple access applications, including cognitive radios. “A Brief History of FBMC Systems” provides a summary of the key developments in this area. The rest of this section expands on these developments in a tutorial style.

### FBMC SYSTEMS FOR QAM SYMBOL TRANSMISSION

Consider a multicarrier data transmission system similar to Figure 1. In OFDM, successive blocks of data symbols  $\{s_k[n], k \in \mathcal{K}\}$ , for different choices of the time index  $n$ , are isolated through the use of CP. In this section, we present a different point of view of the signal model (2) that allows orthogonality of different modulated data symbols without any use of CP. Since CP constitutes a loss of bandwidth efficiency, this method has the potential of achieving a higher bandwidth efficiency than OFDM. Moreover, we recall that time spreading (i.e., a nonzero duration) of channel impulse response leads to frequency selectivity. The dual of this property is that the time variation of a channel results in spreading of the subcarrier spectra, resulting in ICI. Channels with both time and frequency

spreading are called doubly dispersive. An important part of our discussion in this section is devoted to the design of the prototype filters that are robust under doubly dispersive channels. However, before introducing such designs, we first concentrate on channels that only suffer from time spreading (i.e., are time invariant). Examples of such channels are subscriber lines and power lines. This design may also prove very useful in the cases of wireless channels with slow mobility.

Recall (6) and that the data symbols  $s_k[n]$  will be separable if (7) holds. To satisfy (7), in FBMC, the receiver uses a prototype filter  $p_R(t)$  that is matched to the transmit prototype filter  $p_T(t)$ , i.e.,  $p_R(t) = p_T(-t)$ , and  $p_T(t)$  is designed to satisfy the criteria discussed below. Since most of the design methods that have been proposed in the literature consider symmetric prototype filters, i.e.,  $p_T(t) = p_T(-t) = p_R(t)$ , in the rest of this article, we drop the subscripts “T” and “R” and thus use  $p(t)$  to denote a prototype filter that is used for both signal synthesis at the transmitter and signal analysis at the receiver.

### AMBIGUITY FUNCTION AND GENERALIZED NYQUIST CONSTRAINTS

The orthogonality condition (7) and further results to be developed in the rest of this article can be best explained through the ambiguity function of  $p(t)$ , defined as

$$A_p(\tau, \nu) = \int_{-\infty}^{\infty} p(t + \tau/2) p^*(t - \tau/2) e^{-j2\pi\nu t} dt, \quad (18)$$

where  $\tau$  is a time delay and  $\nu$  is a frequency shift. Recalling (5), assuming  $f_k = kF$  and removing the subscripts T and R, one finds that

$$\begin{aligned} \langle p_k(t-mT), p_l(t-nT) \rangle &= \int_{-\infty}^{\infty} p(t-mT) e^{j2\pi kFl} p(t-nT) e^{-j2\pi lFl} dt \\ &\propto A_p((n-m)T, (l-k)F), \end{aligned} \quad (19)$$

where  $\propto$  denotes proportionate to. The proportionate factor is a phase shift due to the delays of  $mT$  and  $nT$ , whose value is irrelevant to our discussion here. Using (19), (7) may be written in terms of the ambiguity function as

$$A_p(nT, lF) = \begin{cases} 1, & n = l = 0, \\ 0, & \text{otherwise.} \end{cases} \quad (20)$$

We note that the case where  $\nu = 0$  corresponds to the familiar (time) correlation function

$$A_p(\tau, 0) = \int_{-\infty}^{\infty} p(t + \tau/2) p(t - \tau/2) dt, \quad (21)$$

which reduces to the Nyquist constraints

$$A_p(nT, 0) = \begin{cases} 1, & n = 0, \\ 0, & \text{otherwise.} \end{cases} \quad (22)$$

Also, one may note that the integral on the right-hand side of (21) is equal to the convolution of  $p(t)$  and its matched pair

## FILTERED OFDM: LIMITATIONS AND OPTIMIZATIONS

From our discussion so far, we have found that the filtering operations in filtered OFDM are based on the prototype filters whose impulse responses are presented in Figure 4. Each of these responses are characterized by a flat top and two transition periods at the beginning and end. Note that the flat top imposed over a significant portion of the impulse responses is a serious design constraint. This constraint is a direct consequence of the fact that the modulation and demodulation in OFDM are based on simple IFFT and FFT operations, respectively. From the design point of view of a filter, the designer has the transition periods only at the beginning and end of the prototype filter to optimize its frequency response. Hence, in practical cases where to keep the bandwidth efficiency of the system high,  $T_0$  and  $T_1$  are selected to be much smaller than  $T$  (and  $T_{\text{FFT}}$ ), one may find that the prototype filters in filtered OFDM suffer from poor magnitude responses. For example, the design example presented in Figure 5 suffers from a wide transition band.

## IMPROVED FILTER DESIGN

So far, the design of filtered OFDM has been limited to the use of raised-cosine pulses that are presented in Figure 4. A fundamental question that one may ask is the following: "Can the raised-cosine pulse shape (which may also be thought of as a window function) be replaced by a pulse shape with an improved frequency domain response?" To provide an answer to this question that will be both informative and constructive, we begin with a graphical presentation of (12), shown in Figure S1. Examining this figure, one may note that the rolloff of the raised-cosine pulse shape is determined by the half-sine wave pulse  $h(t)$ . Moreover, from Figure 5, one may note that the magnitude of the Fourier transform of  $h(t)$  determines the envelope of the magnitude response of the raised-cosine window function  $p_T(t)$ . Obviously, one need not to limit  $h(t)$  to the half-sine wave pulse. Any pulse with the following constraints will satisfy the flat top and finite duration of the roll-off intervals of  $p_T(t)$ :

$$\int_0^{T_0} h(t) dt = 1 \quad \text{and} \quad h(t) = 0, \quad \text{and } t < 0 \text{ for } t > T_0. \quad (S1)$$

Therefore, to design  $h(t)$ , one may define a cost function whose optimization subject to the constraints (S1) leads to a good design.

Since the choice of the cost function is unlimited, many designs are possible. For the sake of exposition, we limit our discussion to the use of the common window functions that are often used to design finite impulse response (FIR) digital filters. We note that  $h(t)$  may be thought of as a window function and the half-sine wave is one particular choice of it. There are many other choices. The commonly used window functions, among others, are rectangular, Hamming, Hanning, and Blackman [60]. These window functions, for a desired window time duration  $0 \leq t \leq T_0$ , have the following closed-form expressions:

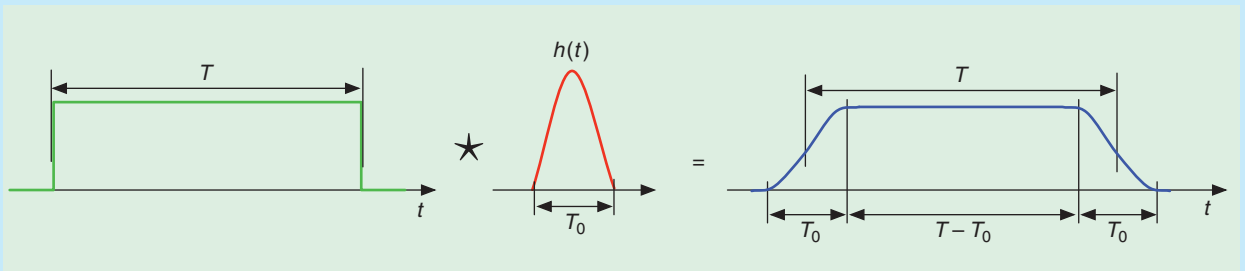
$$\text{Rectangular: } h(t) = K_1 \Pi\left(\frac{t - T_0/2}{T_0}\right),$$

$$\text{Hamming: } h(t) = K_2 \left(0.54 - 0.46 \cos \frac{2\pi t}{T_0}\right) \Pi\left(\frac{t - T_0/2}{T_0}\right),$$

$$\text{Hanning: } h(t) = K_3 \left(0.5 - 0.5 \cos \frac{2\pi t}{T_0}\right) \Pi\left(\frac{t - T_0/2}{T_0}\right),$$

$$\text{Blackman: } h(t) = K_4 \left(0.42 - 0.5 \cos \frac{2\pi t}{T_0} + 0.08 \cos \frac{4\pi t}{T_0}\right) \times \Pi\left(\frac{t - T_0/2}{T_0}\right)$$

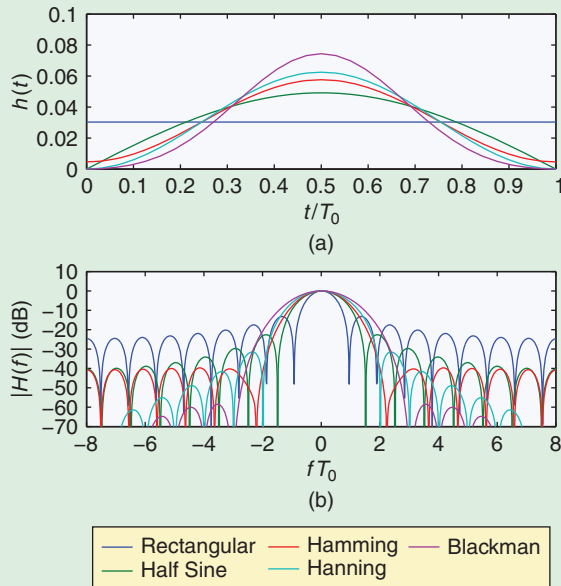
where  $K_1$ – $K_4$  are the normalizing constants that are selected so that constraint (S1) is satisfied. These window functions along with the half-sine wave are presented in Figure S2, in both time and frequency domains. From this figure one can see that, in the frequency domain, while the rectangular window offers the narrowest main lobe, Hamming, Hanning, and



[FIGS1] A graphical presentation of (12).

$p(-t)$ , evaluated at time  $t = \tau$ . Thus,  $A_p(t, 0) = p(t) \star p(-t)$  and, hence (22) implies that  $p(t)$  is a square-root Nyquist pulse [28], [62]. Moreover, the ambiguity function  $A_p(\tau, \nu)$  may be thought of as a generalization of the correlation function

$A_p(\tau, 0)$ , where a correlation is found between  $p(t)$  and its modulated version at the frequency  $f = \nu$ . Accordingly, we refer to the set of constraints (20) as the generalized Nyquist constraints.



**[FIGS2]** Comparison of the rectangular, half-sine-wave, Hamming, Hanning, and Blackman window functions.

Blackman windows offer lower side lobes at the cost of a wider main lobe. This observation shows that one can trade the width of the main lobe of  $|H(f)|$  (equivalent to the transition width of  $|P_T(f)|$ ) with suppression of the out-of-band side lobes. The half-sine-wave window function thus appears to be a good compromised choice.

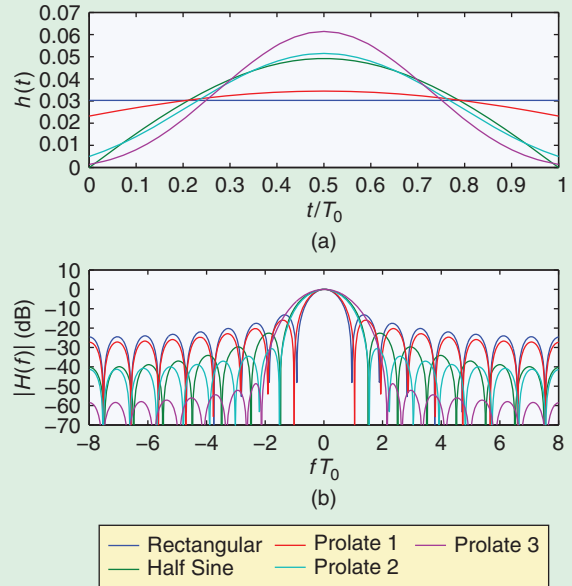
Following the above observation, a question that may arise is: “Can one find a design procedure to allow trading the width of the main lobe of  $|H(f)|$  with the suppression of the side lobes in a systematic way, which results in designs which are optimal in some defined sense?” It turns out that a class of such design exists. They are called prolate windows and their design may be formulated as follows [60], [61].

Given a bandwidth of  $\Delta f$ , stretching over the interval  $-\Delta f/2 < f < \Delta f/2$ , find a time domain function  $h(t)$  that, say, subject to the constraints (S1), minimizes the out-of-band energy of  $H(f)$ , defined as

$$J = \int_{-\infty}^{\infty} |H(f)|^2 df - \int_{-\Delta f/2}^{\Delta f/2} |H(f)|^2 df. \quad (S2)$$

This problem can be solved numerically as follows [61]:

- Choose a sampling frequency  $f_s \gg \Delta f$  and define the normalized equivalent of  $\Delta f$  as  $\Delta f_N = \Delta f/f_s$ .
- Consider a random process  $x[n]$  with the power spectral density. (We use  $n$ , in square brackets, to denote the discrete time index.)



**[FIGS3]** Comparison of a set of prolate window designs with the rectangular and half-sine-wave window functions. Prolate designs 1 and 2 have been aimed at achieving main lobes that are close to those of rectangular and half-sine-wave windows, respectively. In both cases, the side lobes of the prolate designs are lower.

$$\Phi_{xx}(e^{j2\pi f_N}) = \begin{cases} 1, & |f_N| < \Delta f_N/2, \\ 0, & \text{otherwise,} \end{cases} \quad (S3)$$

where  $f_N$  is the normalized frequency with the range of  $-0.5 \leq f_N \leq 0.5$ .

- Construct an  $M$ -by- $M$  correlation matrix  $\mathbf{R}$  of  $x[n]$ , where  $M = T_0 f_s$ . This is the symmetric Toeplitz matrix whose first row consists of the autocorrelation coefficients of  $x[n]$ , viz.,  $\phi[k] = \Delta f \text{sinc}(\Delta f_N k)$ , for  $k = 0, 1, \dots, M-1$ .
- The eigenvector of  $\mathbf{R}$  that corresponds to its maximum eigenvalue is the desired window function. Note that, as desired, it has the length of  $MT_s = T_0$ , where  $T_s = 1/f_s$ .

The above procedure can be easily programmed into any numerical programming package. Figure S3 presents the results of three designs of prolate window functions in both time and frequency domains. The rectangular and half-sine-wave window functions are also presented for comparison. The first and second prolate windows are designed to match, respectively, the main lobes of the rectangular and half-sine-wave windows closely. The second prolate design, in particular, has a main lobe that overlaps with that of the half-sine-wave window almost perfectly. However, its first few side lobes are significantly lower than their counterparts in the half-sine-wave window function.

## FILTER DESIGN METHODS (PRELIMINARY DESIGNS)

A number of methods may be adopted to design a prototype filter  $p(t)$  that satisfies the generalized Nyquist constraints (20), exactly or within some acceptable approximation.

A naive approach, but still effective for time-invariant or slowly time-varying channels, is to design  $p(t)$  to be a square-root Nyquist filter that satisfies the constraints (22) and, at the same time, limits the pass and transition bands (the support interval)



## A BRIEF HISTORY OF FBMC SYSTEMS

The pioneering work on FBMC communication techniques was done by Chang [8] and Saltzberg [9] in the mid 1960s. Chang presented the conditions required for signaling a parallel set of PAM symbol sequences through a bank of overlapping filters within a minimum bandwidth. To transmit PAM symbols in a bandwidth-efficient manner, Chang proposed vestigial sideband (VSB) signaling for subcarrier sequences. Saltzberg extended the idea and showed how Chang's method could be modified for transmission of QAM symbols in a double-sideband (DSB)-modulated format. Efficient digital implementation of Saltzberg's multicarrier system through polyphase structures was first introduced by Bellanger [11] and later studied by Hirosaki [12]. Another key development appeared in [52], where the authors noted that Chang's/Saltzberg's method could be adopted to match channel variations in doubly dispersive channels, hence, minimize ISI and ICI. This point, which is extensively elaborated on in this article, can lead to a significant improvement of FBMC over OFDM in highly mobile channels.

In the 1990s, advancements in DSL technology motivated more activity beyond discrete multitone (DMT), the equivalent terminology often used in DSL literature instead of OFDM. Early development in this area is an American National Standards Institute (ANSI) contribution by Sandberg

and Tzannes, which was later expanded and called discrete wavelet multitone (DWTM) [40]. Although the connection between DWTM and early developments of FBMC remained unnoticed for many years, more recent studies have revealed that DWTM is closely related to Chang's method [8]. Farhang-Boroujeny and Yuen [30], in particular, have viewed DWTM as a reinvention of Chang's method. Despite its great advantages over OFDM (in suppressing narrow-band interferences), unfortunately, the relatively complex equalizer structure adopted in [40] kept the industry lukewarm in adopting DWTM. Later, the researchers found alternative/simpler solutions to channel equalization in DWTM, e.g., [32], and, hence, DWTM was seriously considered for adoption in standards, e.g., [50].

Filtered multitone (FMT) is another multicarrier modulation technique that has been specifically developed for DSL applications [43]–[45]. As opposed to the FBMC methods that follow the original idea of Chang and Saltzberg, allowing the overlapping of adjacent subcarrier bands to maximize the bandwidth efficiency, FMT follows the conventional method of frequency division multiplexing; thus, the subcarrier bands are separated by guard (their transition) bands. Hence, FMT is less bandwidth efficient than the FBMC methods proposed by Chang and Saltzberg. Nevertheless, as discussed in this article, FMT offers advantages in certain applications.

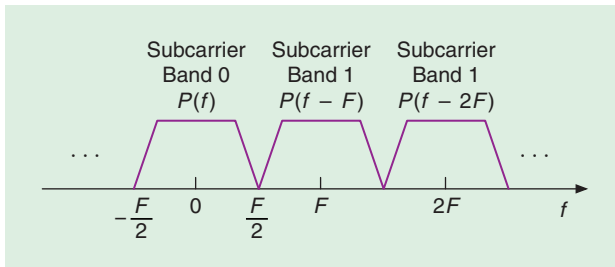


**[FIG6]** Spectra of a set of subcarrier signals with support intervals  $((k - 0.5)F, (k + 0.5)F)$ , for  $k = 0, 1, 2, \dots$

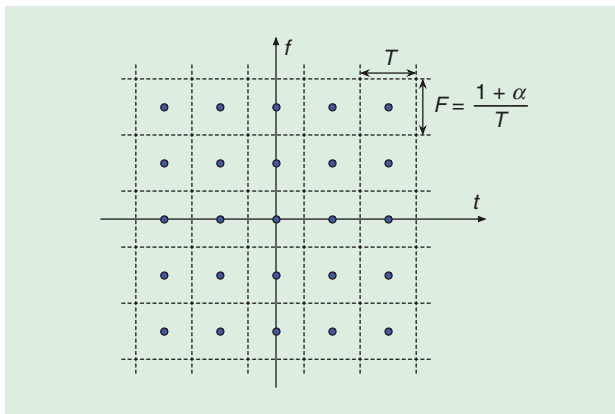


**[FIG7]** Time-frequency phase-space lattice representation in an FBMC system. The parameter  $\alpha$  is the roll-off factor of the prototype square-root Nyquist filter. Symbol density =  $1/TF = 1/(1 + \alpha)$ .

of  $P(f)$  to the limited interval  $(-F/2, +F/2)$ . This is demonstrated in Figure 6. Clearly, the fact that the spectra of different subcarrier channels are nonoverlapping implies that there is no ICI. From the ambiguity function point of view, considering the support interval of  $P(f)$ , it is straightforward to show that  $A_p(\tau, \nu) = 0$  for  $|\nu| \geq F$ . This, in turn, implies that the constraints  $A_p(nT, lF) = 0$  are satisfied for all nonzero values of  $l$ . The rest of the constraints in (20), i.e., the case where  $l = 0$ , are satisfied, since  $p(t)$  is a square-root Nyquist filter.

Figure 7 presents a grid of time-frequency points of the transmitted data symbols, i.e., the corresponding time-frequency phase-space lattice. From this, one finds that there is one symbol in each  $TF$  unit area. This leads to a symbol density

$$\frac{1}{TF} = \frac{1}{1 + \alpha} \leq 1. \quad (23)$$

In Figure 7 and (23),  $\alpha$  is the roll-off factor parameter, commonly used in the design of pulse shapes (transmit and receive filters) in communication systems [62].

At this point, it is instructive to compare (11) and (23) and also the time-frequency phase-space lattices presented in Figures 3 and 7. We recall that, in the case of FBMC,  $T = T_{\text{FFT}}$ , however, in OFDM,  $T > T_{\text{FFT}}$ . Then, obviously, OFDM and FBMC systems will have the same bandwidth efficiency if  $1 + \alpha = T/T_{\text{FFT}}$ . Hence, for instance, if in OFDM  $T/T_{\text{FFT}} = 1.25$ , i.e., the length of CP is one quarter of the FFT length, to implement an FBMC system with the same bandwidth efficiency, one should set  $\alpha = 0.25$ .

It is also worth noting that in the setup discussed above, an FBMC uses a set of filters that have no overlap (see Figure 6). This clearly follows the principle of the classical frequency division multiplexing (FDM). Later, we will discuss the other FBMC setups in which the adjacent subcarriers are allowed to overlap and, thus, can achieve the maximum bandwidth efficiency of one. Nevertheless, we note that the use of FBMC systems with nonoverlapping subcarrier bands has been proposed and studied by a number of researchers. In fact, FMT that has been proposed for communication over DSLs uses filter banks with nonoverlapping subcarriers. See “A Brief History of FBMC Systems” and the relevant discussions in the section “Activities in the Standard Committees.”

### AMBIGUITY SURFACE

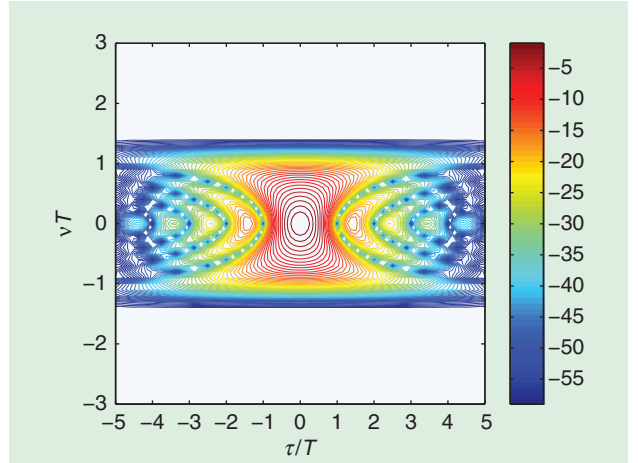
An instructive method of looking at the ambiguity function is that it indicates how each symbol is spread across the time and frequency axes. Regular zero crossings of the ambiguity function  $A_p(\tau, \nu)$  at the grid points  $\tau = nT$  and  $\nu = lF$  for nonzero integer values of  $n$  and  $l$  guarantee ISI- and ICI-free transmission when the channel is ideal. However, spreading the modulated signals along the time and frequency axes may be interpreted as some blurring effect on the ambiguity function that are caused by superposition of multiple copies of the ambiguity functions that have shifted with respect to each other as a result of presence of multipaths (spreading in time) and multi-Doppler shifts (spreading in frequency). The impact of this effect can be best understood by visualizing a three-dimensional plot of the ambiguity function  $A_p(\tau, \nu)$ . We refer to such plots as ambiguity surface.

Figure 8 presents an example of the ambiguity surface, using a set of contour plots. Here,  $p(t)$  is a square-root-raised cosine filter with a roll-off factor,  $\alpha$ , given by

$$p(t) = \frac{\sin\left((1-\alpha)\frac{\pi t}{T}\right) + \frac{4\alpha t}{T} \cos\left((1+\alpha)\frac{\pi t}{T}\right)}{\frac{\pi t}{T} \left(1 - \left(\frac{4\alpha t}{T}\right)^2\right)}. \quad (24)$$

Clearly, ICI is avoided if  $F$  is given any value greater than  $(1+\alpha)/T$ . We may also note that the ambiguity function reaches a level of  $-50$  dB or lower at the points  $\tau/T = \pm 1, \pm 2, \dots$  and  $\nu = 0$ ; the blue dots along the line  $\nu = 0$ . This is related to the fact that the data symbols that are spaced at the regular time interval  $T$  do not interfere with each other, which means that ISI-free transmission has been established.

Theoretically, it is possible to design a prototype filter with an excess bandwidth of zero, i.e., with parameter  $\alpha = 0$ . In that case,  $F$  may be set equal to  $1/T$ . This leads to a maximum density  $1/TF = 1$ . However, we note that the choice of  $\alpha = 0$  leads to a number of practical difficulties that render it impossible to achieve in practice. In particular,  $p(t)$  remains significant over many (tens of) symbol intervals. This leads to the following practical problems:



**[FIG8]** Ambiguity surface of a square-root raised-cosine filter for a roll-off factor  $\alpha = 0.5$ . The white spaces in the regions  $|\nu| > 1.5$  are the areas where  $|A(\tau, \nu)| < 0.001$  (i.e., it is below  $-60$  dB).

- The very long length of  $p(t)$  adds significant complexity to the transmitter and receiver, which uses samples of  $p(t)$  for the realization of the respective synthesis and analysis filter banks.
- Any timing offset at the receiver (or time spreading, arising from multipath effects in channel) results in a large number of ISI terms, which may add up and lead to a significant ISI power.
- In time-varying channels, a long length of  $p(t)$  is problematic as the addition of a multiplicative term (the channel gain) to each transmitted pulse  $p(t)$  results in a new pulse (say,  $q(t) = p(t)c(t)$ , where  $c(t)$  is the channel gain) that may no longer be orthogonal to the time- and frequency-shifted replicas of  $p(t)$ . This can result in a significant amount of ISI and ICI.

The above problems persist (in one way or another) even in cases where  $\alpha > 0$  but reduce as  $\alpha$  increases.

In the past, many researchers have noted these shortcomings of the square-root Nyquist designs and, as a result, have taken a different approach to design prototype filters for FBMC systems. These elegant filter design methods are discussed next.

### FILTER DESIGN METHODS (ADVANCED DESIGNS)

To design prototype filters that address both time and frequency dispersions, it has been argued [52] that one should choose a pulse-shape  $p(t)$  whose time and frequency dispersions matches those of the channel. For this purpose, one may define the dispersion of  $p(t)$  and  $P(f)$ , respectively, as

$$\sigma_t = \sqrt{\int_{-\infty}^{\infty} t^2 |p(t)|^2 dt} \quad (25)$$

and

$$\sigma_f = \sqrt{\int_{-\infty}^{\infty} f^2 |P(f)|^2 df}. \quad (26)$$

On the other hand, the channel time and frequency dispersion are, respectively, quantified by  $\Delta\tau$  (a measure of the duration of the channel impulse response) and  $\Delta\nu$  (a measure of the range of the channel Doppler shift). To match the prototype filter with these loosely defined quantities, it is intuitively sound to choose  $p(t)$  such that the following identity holds [52]:

$$\frac{\sigma_t}{\Delta\tau} = \frac{\sigma_f}{\Delta\nu}. \quad (27)$$

Moreover, it has been noted that since time and frequency may be thought as a pair of dual variables, a reasonable choice of  $p(t)$  is the one with the following property:

$$P(f) = p(\eta f), \quad \text{for a constant scaling factor } \eta, \quad (28)$$

i.e., a function that has the same form in both the time and frequency domains.

Now, if  $p(t)$  is designed to satisfy (28) and be a square-root Nyquist filter in which the zero crossings of  $p(t) \star p(t)$  are at an interval  $T$ ,  $P(f) \star P(f)$  also has regular zero crossings at an interval  $F$ , and  $T/F = \eta$ . In that case, (27) may be written as

$$\frac{T}{\Delta\tau} = \frac{F}{\Delta\nu}$$

or

$$\frac{T}{F} = \frac{\Delta\tau}{\Delta\nu} = \frac{\sigma_t}{\sigma_f} = \eta. \quad (29)$$

Accordingly, to maximize the symbol density  $1/TF$ , one should choose to minimize the time-delay spread product  $\sigma_t \sigma_f$ . On the other hand, the Heisenberg–Gabor uncertainty principle states that [63]

$$\sigma_t \sigma_f \geq \frac{1}{4\pi}, \quad (30)$$

where the equality holds only when  $p(t)$  is equal to the Gaussian pulse

$$g(t) = e^{-\pi t^2}. \quad (31)$$

Also, the Gaussian pulse  $g(t)$  has an interesting property that  $G(f) = g(f)$ , i.e., it satisfies the desirable property (28), with  $\eta = 1$ . However,  $p(t) = g(t)$  does not satisfy the orthogonality conditions (20).

Attempts to design filters that satisfy the orthogonality conditions (20), and at the same time approach the Heisenberg–Gabor uncertainty lower bound (30) as close as possible, have been made, and design methods have been developed [52], [54]. The isotropic orthogonal transform algorithm (IOTA) prototype filter design is the most popular method [52].

IOTA design/algorithm was first introduced by Alard [53] and was put in archival journals by Le Floch et al. [52]. The algorithm starts with the Gaussian pulse  $g(t) = e^{-\pi t^2}$  and converts it to the orthogonalized pulse

$$p_N(t) = \mathcal{F}^{-1} \mathcal{O}_{\tau_0} \mathcal{F} \mathcal{O}_{\nu_0} g(t), \quad (32)$$

where the parameters  $\tau_0$  and  $\nu_0$  are defined below,  $\mathcal{F}$  and  $\mathcal{F}^{-1}$ , respectively, denote the Fourier and inverse Fourier transforms, and  $\mathcal{O}_a$  is an orthogonalization operator defined as

$$y(u) = \frac{x(u)}{\sqrt{\frac{1}{a} \sum_{k=-\infty}^{\infty} |x(u - k/a)|^2}}. \quad (33)$$

The orthogonalization step  $\mathcal{O}_{\nu_0}$  introduces nulls in the ambiguity function  $A_{p_N}(\tau, \nu)$  at the frequency points  $\nu = \pm\nu_0, \pm 2\nu_0, \pm 3\nu_0, \dots$ , and  $\mathcal{O}_{\tau_0}$  introduces nulls at the time points  $\tau = \pm\tau_0, \pm 2\tau_0, \pm 3\tau_0, \dots$ . Because of the reasons that will become clear shortly, we refer to  $p_N(t)$  as a (time/frequency)-normalized prototype filter.

The choice of  $\tau_0$  and  $\nu_0$  is somewhat arbitrary. However, any time scaling of  $p_N(t)$  to convert it to a pulse  $p(t)$  with a zero-crossing interval  $T$  will also amend the zero crossings of  $P_N(f)$  to  $F$ , and the identity  $TF = \tau_0\nu_0$  always holds. On the other hand, since  $1/TF$  is the density of the multicarrier symbols, one may note that the density of the multicarrier symbols can also be evaluated as  $1/(\tau_0\nu_0)$ . Moreover, we note that the maximum density  $1/(\tau_0\nu_0) = 1$  is achieved in the case of OFDM when the transmitter and receiver prototype filters (windows) are rectangular and  $T = T_{\text{FFT}}$ . This corresponds to the case where CP could be removed; the case that could only be achieved if the channel was ideal. In the case of FBMC,  $1/(\tau_0\nu_0) = 1$  is only asymptotically achievable, e.g., when the roll-off factor  $\alpha$  of the prototype filters approaches zero. However, fortunately, as will be discussed in the following section, the particular choice of  $1/(\tau_0\nu_0) = 0.5$  (or,  $\tau_0\nu_0 = 2$ ) and a modification to the orthogonality definition (7) lead to a class of FBMC systems with a maximum density of two real-valued symbols (equivalent to one complex-valued symbol) per unit area of the time–frequency phase-space lattice. Moreover, it is convenient to set  $\tau_0 = \nu_0 = \sqrt{2}$ . The ambiguity surface of a normalized prototype filter  $p_N(t)$  that is designed using these parameters is presented in Figure 9.

We refer to  $p_N(t)$  as a normalized prototype filter because zero crossings of its ambiguity function occur at the normalized points  $\tau, \nu = \pm\sqrt{2}, \pm 2\sqrt{2}, \dots$ . The filter  $p(t)$  whose ambiguity function has zero crossings at the points  $\pm T, \pm 2T, \dots$  along the time axis can be readily obtained through a time scaling of  $p_N(t)$ , viz.,  $p(t) = p_N(t\sqrt{2}/T)$ . The zero crossings of  $A_p(\tau, \nu)$  along the frequency axis will then occur at  $\pm F, \pm 2F, \dots$ , with  $F = 2/T$ . We may also note that once the ratio  $\Delta\tau/\Delta\nu = \eta$  is known, recalling (29), one may solve the pair of equations  $T/F = \eta$  and  $TF = 2$ , to obtain  $T = \sqrt{2\eta}$ . Designs with values of  $1 < TF < 2$  are also possible and follow similarly.

## FBMC SYSTEMS FOR PAM SYMBOL TRANSMISSION

When data symbols  $s_k[n]$  are real-valued, i.e., are from a PAM constellation, under certain conditions that will be discussed in this section, the symbol rate can be doubled and also the

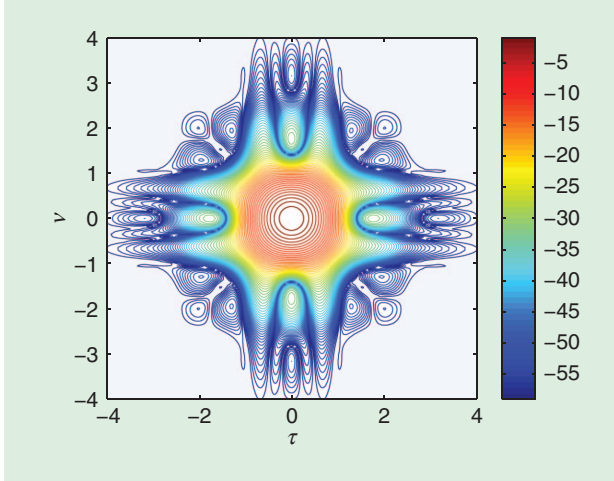


**[FIG9]** Ambiguity surface of a normalized IOTA filter with parameters  $\tau_0 = \nu_0 = \sqrt{2}$ . The white spaces around the surface are the areas where  $|A(\tau, \nu)| < 0.001$  (i.e., it is below  $-60$  dB).

symbol spacing along the frequency axis can be halved. This is equivalent to saying that the density of data symbols in the time–frequency phase-space lattice can be quadrupled. However, noting that each PAM symbol carries one half of information content of each QAM symbol, we can say that the PAM transmission can achieve a data symbol density which is twice that of QAM transmission.

To explain how this increase in the density is achieved, we introduce the transmit signal

$$x(t) = \sum_n \sum_{k \in \mathcal{K}} s_k[n] p_k(t - nT/2), \quad (34)$$

where data symbols  $s_k[n]$ s are real-valued and

$$p_k(t) = p(t) e^{j\pi k F t} e^{j(k+n)\frac{\pi}{2}}. \quad (35)$$

Note that, here, the data symbols are spaced at  $T/2$  along the time axis and at  $F/2$  along the frequency axis. We may also note that the term  $e^{j(k+n)\pi/2}$  in (35) is equivalent to a phase shift that is effectively zero when  $k+n$  is an even number and is  $\pi/2$  when  $k+n$  is an odd number. (We consider any phase value which is an integer factor of  $\pi$  as zero, since it preserves the real-valued nature of PAM symbols, and any phase value which is an odd factor  $\pi/2$  as  $\pi/2$ , noting that it converts the real-valued PAM symbols to a set of imaginary symbols.) This concept is demonstrated through a time–frequency phase-space lattice presentation in Figure 10(a), where the blue dots denote phase shifts of zero and the orange dots denote phase shifts of  $\pi/2$ .

The fact that the PAM data symbols  $s_k[n]$  can be extracted from the signal  $x(t)$  in (34) is based on the following modification to the orthogonality condition (7) [52]:

$$\langle p_k(t - mT/2), p_l(t - nT/2) \rangle = \delta_{kl} \delta_{mn}, \quad (36)$$

where

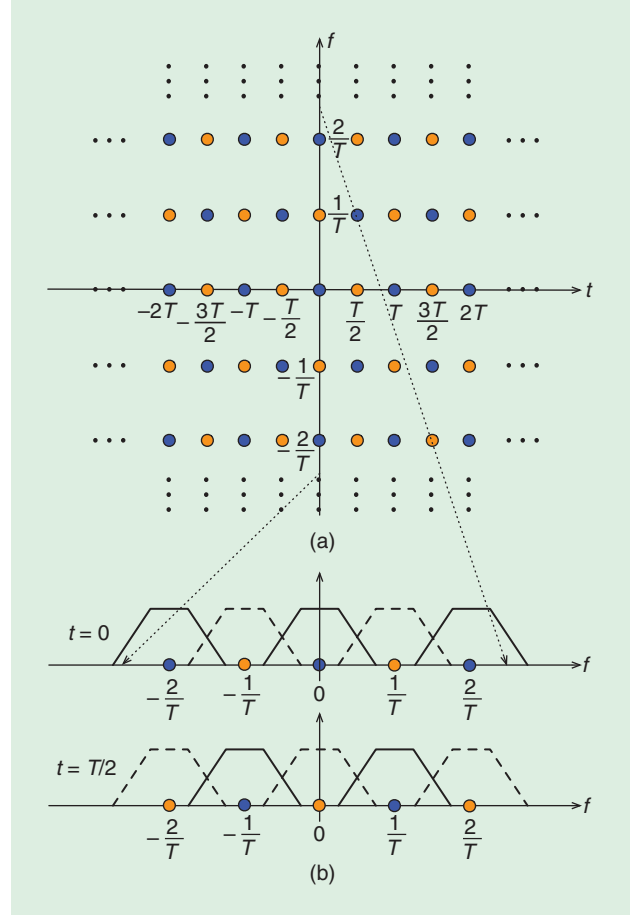


**[FIG10]** (a) A time–frequency phase-space lattice representation of a set of real-valued (PAM) data symbols according to (37). (b) Demonstration of the subcarriers spectra for  $t = 0$  and  $t = T/2$ .

$$\langle p_k(t - mT/2), p_l(t - nT/2) \rangle = \Re \left\{ \int_{-\infty}^{\infty} p_k(t - mT/2) p_l^*(t - nT/2) dt \right\}, \quad (37)$$

and  $\Re\{\cdot\}$  denotes the real part. Note that this modification is based on three changes: 1) following (34), the symbol spacing  $T$  is replaced by  $T/2$ ; 2) from (35), it follows that the carrier spacing  $F$  is replaced by  $F/2$ ; and 3) according to (37), the orthogonality is defined by the real part of the inner product of the underlying functions.

Obviously, when  $p(t)$  is designed according to the procedure discussed above, (36) holds when  $k, l, m$ , and  $n$  are all even numbers. On the other hand, it is not difficult to show that when one or more of the time or frequency indices  $k, l, m, n$  are odd, the only condition necessary for (36) to be true is to have an even-symmetric prototype filter  $p(t)$ , i.e.,  $p(-t) = p(t)$ ; e.g., see [9] and [30]. Therefore, to guarantee the orthogonality condition (36), it is sufficient to add an even-symmetric constraint to  $p(t)$  in addition to those in (7).

Figure 11 presents a possible system structure that synthesizes/modulates a multicarrier signal according to (34). The associated demodulator is also presented. In the literature, this



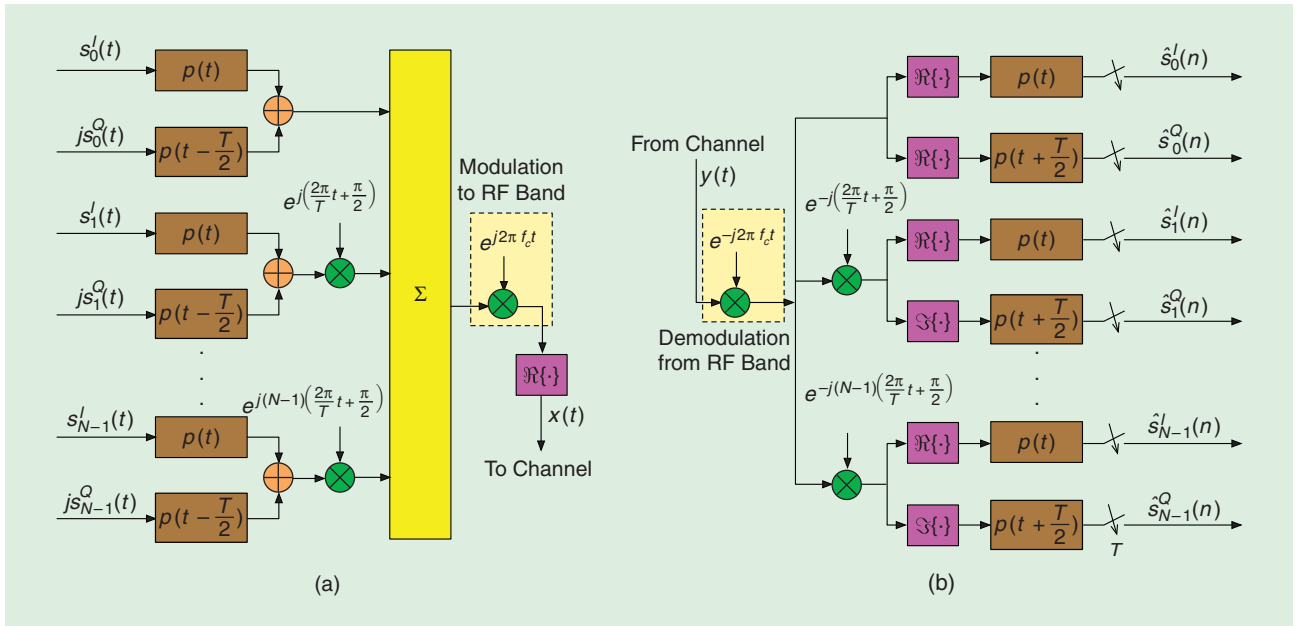


**[FIG11]** A block diagram of an FBMC system using OQAM symbols: SMT.

structure has often been referred to as OFDM-OQAM, where OQAM stands for offset QAM. The more concise name, staggered multitone (SMT), has recently been suggested in [30]. We use this in the rest of this article. At the transmitter, each QAM symbol  $s_k[n]$  is divided into its in-phase (real part),  $s_k^I[n]$ , and quadrature (imaginary part),  $s_k^Q[n]$ , components. These may be thought of as the elements of a pair of PAM sequences that are then transmitted with a time offset  $T/2$ . The time offset  $T/2$  is realized by using a pair of prototype filters denoted by  $p(t)$  and  $p(t - T/2)$ . The phase shift  $\pi/2$  between any pair of adjacent PAM symbols (along the time and frequency axes) is realized by adding the factor  $j = \sqrt{-1}$  to the filter  $p(t - T/2)$  and introducing an additional phase  $\pi/2$  in the modulator block  $e^{jk(2\pi/T)t + (\pi/2)}$ . Modulation from baseband to a radio frequency (RF) band and demodulation to baseband are also shown for completeness.

The spectra of subcarrier signals at time instants  $t = 0$  and  $t = T/2$  are presented in Figure 10(b). Subcarriers are modulated to frequencies  $0, \pm 1/T, \pm 2/T, \dots$ , and the phase difference  $\pi/2$  is introduced to adjacent symbols across time and frequency. The full-line spectra are the symbols that are subject to a phase shift that is an even factor of  $\pi/2$ , and the dashed-line spectra indicate the symbols that are subject to a phase shift that is an odd factor of  $\pi/2$ . We also note that each PAM symbol is subject to a DSB modulation process.

To emphasize and make sure that the distinction between SMT and the alternative method that is introduced next will be clear, we summarize the results that were just developed. SMT is based on a multicarrier modulation of a set of QAM data symbols whose in-phase and quadrature components are time offset with respect to each other by one half of a symbol interval. The pioneering work on SMT

is due to Saltzberg [9]; see “A Brief History of FBMC Systems.” Saltzberg’s work was a followup to the more original work of Chang [8], who had proposed a signaling method for transmission of a parallel set of PAM symbol sequences using a bank of VSB-modulated signals. Figure 12 presents the time–frequency phase-space lattice representation of Chang’s method along with the spectra of the modulated signals at time instants  $t = 0$  and  $t = T$ . The VSB feature of the modulated subcarrier signals is highlighted in Figure 12(b). As noted earlier, Chang’s method has been reformulated and presented under the name DWMT. DWMT, on the other hand, has its origin from cosine-modulated filter banks (CMFB) that were invented and widely used for signal compression [61]. Hence, the alternative name CMFB-OFDM that has appeared in the literature [32] is a synonym to DWMT, and both are closely related to Chang’s method. The more concise name cosine-modulated multi-tone (CMT) was later suggested in [42]. In the rest of this article, we use CMT to refer to discrete-time implementations of Chang’s method.

To better understand the relationship between SMT and CMT, we compare Figures 10 and 12. In terms of symbol density in the time–frequency phase-space lattice, both methods offer a density of two PAM symbols (equivalent to one QAM symbol) per unit area; for SMT, density =  $1/((T/2) \times (1/T)) = 2$ , and for CMT, density =  $1/((T) \times (1/2T)) = 2$ . Also, Figure 12 can be obtained from Figure 10 by scaling the time by a factor of two and, accordingly, the frequency by a factor of 0.5 and then shifting the points in the direction of frequency by  $1/4T$ . This, as can be seen from the spectra in Figure 12(b), is equivalent to replacing the DSB spectra in Figure 10(b) by a set of VSB spectra. A formal mathematical derivation of the relationship

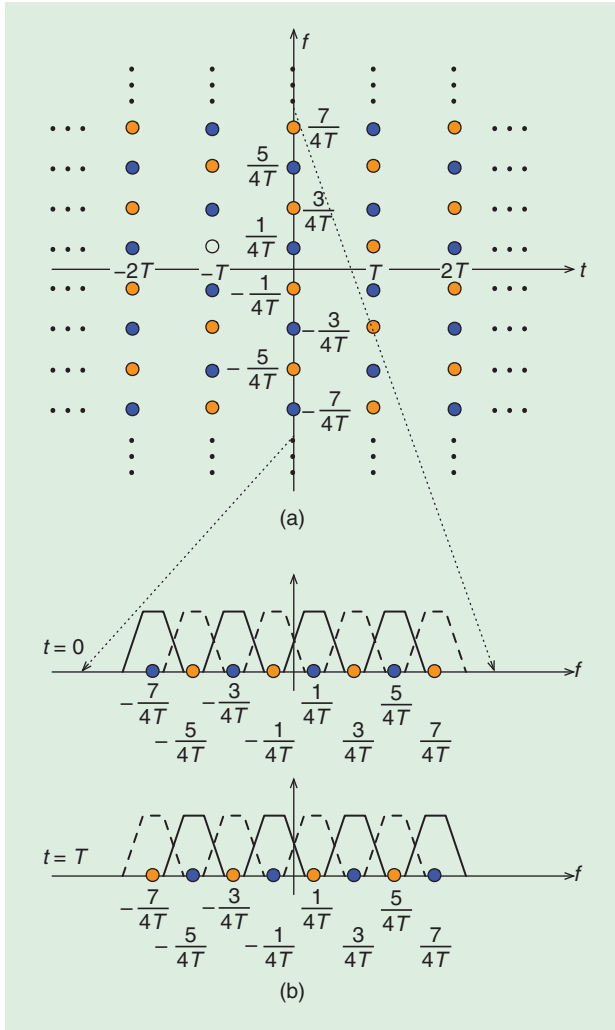


**[FIG12]** (a) A time–frequency phase-space lattice representation of Chang’s modulation method/CMT. (b) Demonstration of VSB modulation in CMT.

between SMT and CMT that leads to these results has recently been reported in [30].

Figure 13 presents a block diagram of a CMT modem. The VSB modulations are established through the modulated filters  $p(t)e^{j(\pi/2T)t}$ . It can be shown, [30], that when  $p(t)$  is a square-root Nyquist filter that is designed such that the zero crossings of  $p(t) \star p(t)$  are at the regular interval  $2T$ , the filter  $p(t)e^{j(\pi/2T)t}$  leads to a VSB modulation of a PAM sequence with the symbol spacing  $T$ .

### COMPLEXITY ISSUES AND POLYPHASE IMPLEMENTATIONS

During the early phase of development of multicarrier systems, industry was reluctant to adopt FBMC, partly because of its perceived high computational complexity. For instance, the first proposal on the use of CMT in the DSL technologies (called DWMT in DSL literature [40]) adopted an equalizer structure that was rather complex; more details are given in the section “Activities in the Standard Committees.” It was later shown that per subcarrier equalization in FBMC systems can be as simple as their counterparts in OFDM, viz., a single complex tap per subcarrier in most practical cases is sufficient, e.g., see the next subsection. Moreover, the use of polyphase structures leads to efficient implementations of FBMC systems; e.g., see [12] for some early developments in this area. Here, we make the general comment that the basic structure of an FBMC system is more complex (but not significantly) than its OFDM counterpart. However, when OFDM is applied to multiple access applications in the uplink of a network, the advanced cancellation techniques that may have to be adopted to combat interference among signals from different users can increase the complexity of OFDM significantly, and hence, it may surpass the complexity of FBMC. More details are given in the section “Multiple Access Communications.”

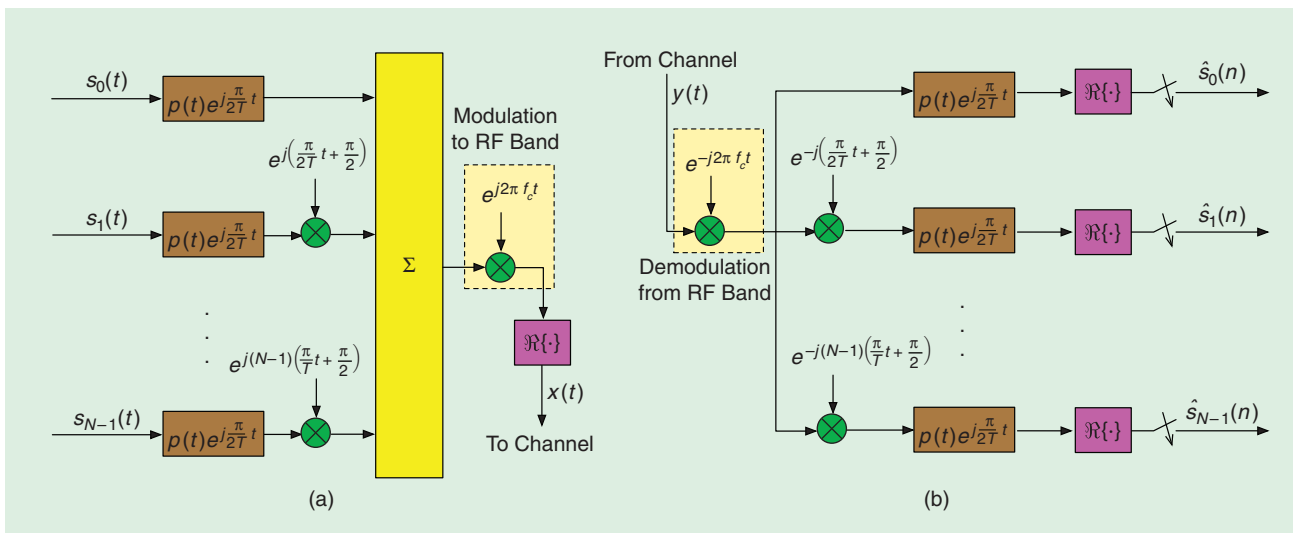


**[FIG13]** A block diagram of an FBMC system using VSB modulation signaling: CMT.

## OFDM VERSUS FBMC IN VARIOUS APPLICATIONS

*Single-user communications:* OFDM offers a lower complexity. FBMC offers a higher bandwidth efficiency.

*MIMO communications:* OFDM provides full flexibility. FBMC can be used in certain MIMO setups. Only FMT can offer the same flexibility as OFDM. But, FMT suffers from the same bandwidth loss as OFDM.

*Multiple-access communications:* In downlink, OFDM offers lower complexity, while FBMC provides higher bandwidth efficiency. In uplink, synchronization among signals from different nodes is required for proper operation of OFDM. In addition, since under mobility conditions, perfect synchronization is not possible, interference cancellation techniques are necessary. Synchronization requirement in an FBMC network is less stringent, and no cancellation technique is necessary. Because of the complexity requirement of interference cancellation, in the uplink of a mobile multiple access network, OFDM has a higher complexity than FBMC.

*Cognitive-radio communications:* Excellent filtering of subcarriers in FBMC makes it an ideal choice for cognitive radios. OFDM/filtered OFDM is a poor fit.

*Doubly dispersive channels:* FBMC can be optimized to match doubly dispersive channels. OFDM/filtered OFDM is a poor fit.

*DSL and PLCs:* Excellent filtering of subcarriers in FBMC makes it an ideal choice for these applications. Filtered OFDM is a less ideal choice. OFDM is a poor fit. FBMC is more complex than OFDM/filtered OFDM.

## EQUALIZATION

The derivations and discussions so far were based on the assumption that the channel was ideal, i.e., a channel with a constant gain and a constant group delay across the frequency band that includes all the subcarrier channels. However, we note that the main reason for using any multicarrier technique, including FBMC systems, is to deal with frequency-selective channels, i.e., the channels whose gain vary across the frequency band and thus may suffer from a significant level of ISI and ICI. On the other hand, the most important advantage of multicarrier techniques is that they greatly simplify the task of channel equalization, a mechanism that is used to combat ISI and ICI. In a single-carrier system, when the channel suffers from a significant level of ISI, a transversal/FIR filter with many taps has to be used to generate a response that resembles the inverse of the channel gain across the transmission band. Such inversion will result in a noise enhancement across the portion of the frequency band for which the channel gain is low. Adaptation of the equalizer tap weights also may not be a straightforward task. Wireless multipath channels are always time varying, and thus the equalizer should be adapted to track channel variations. The speed of tracking decreases as the length of equalizer increases [69]. Hence, when the channel is highly frequency selective and as a result a long equalizer has to be

used, an equalizer adaptation algorithm may not be able to cope with the channel variation.

The above problems are solved or at least greatly moderated when a multicarrier method is adopted. In the case of OFDM, as long as the duration of the channel impulse response is shorter than the CP length and channel variation over each OFDM symbol is negligible, a frequency-selective channel converts to a number of subcarrier channels with flat gains. In FBMC, the assumption of a flat gain over each subcarrier channel is true only approximately. However, the accuracy of this approximation improves as the bandwidth of each subcarrier channel decreases. Here, the bandwidth is defined as a frequency range that includes the pass and transition bands of each subcarrier channel.

Like OFDM, equalization is also performed in FBMC systems separately on each subcarrier channel. Hirosaki [12] explored the case where each subcarrier band within an FBMC system could not be approximated by a flat gain. He showed that, in such cases, to preserve the orthogonality of each subcarrier channel with its adjacent bands, the equalizer at each subcarrier channel should be a fractionally spaced one. The sampling at each subcarrier channel should be equal to the total bandwidth of the respective subcarrier signal. This, in the case of the Nyquist prototype filter that was presented earlier, results in a  $T/2$ -spaced equalizer. In the cases of IOTA filters, equalizers with more closely spaced taps may be required, since these filters have wider bandwidths than their Nyquist counterpart. However, if the number of subcarriers is sufficiently increased so that each subcarrier band could be approximated by a flat gain, a single-tap equalizer per subcarrier will suffice [32], and this will be applicable to all cases irrespective of the prototype filter design.

## APPLICATIONS

To put the results of the previous sections in a prospect of future communication systems, a number of applications of multicarrier systems are reviewed in this section. This review is meant to highlight the advantages of OFDM that has made it the choice for many of the past communication systems and also to discuss some of its shortcomings in future developments. The pros and cons of FBMC in each application is also discussed. A summary of the observations made in this section are presented in "OFDM Versus FBMC in Various Applications."

### SINGLE-USER COMMUNICATIONS

By single user, we refer to the case where a full multicarrier band is available for data transmission between two nodes. In that case, the transmitter generates all subcarrier signals simultaneously and synchronously. Also, following the modulation type (being OFDM or FBMC), the receiver can perform the necessary carrier and timing recovery actions and decode the transmitted information. The key point here is that all signals within the band of interest are jointly synthesized and thus are perfectly synchronized with one another. Therefore, either the OFDM

or FBMC method can be adopted. The selection of one against the other is a designer choice.

On one hand, OFDM offers the advantages of 1) lower complexity and 2) robust performance with respect to timing-phase error; the presence of CP allows some variation of timing phase without any adverse effect on the system performance. On the other hand, FBMC methods offer the advantage of higher bandwidth efficiency because of the absence of CP samples.

### **MIMO COMMUNICATIONS**

Communication systems that employ multiple antennas at both the transmitter and receiver (called MIMO) to increase the system throughput and the reliability of the link have become very popular in the past decade and have been included in most of the recent standards. It turns out that while the application of OFDM to MIMO channels is a straightforward task, direct application of FBMC to MIMO channels may not be possible in general. Assuming that the channel could be approximated by a flat gain over each subcarrier band, FMT application to MIMO channels is straightforward. However, application of the more bandwidth-efficient structures that are presented in Figures 11 and 13 to MIMO channels is nontrivial. As of today, some limited studies have been reported in [70] and [71]; however, these are only for very specific applications. The general understanding is that only FMT-based FBMC systems can offer the same flexibility as OFDM in adopting the various MIMO techniques.

### **MULTIPLE ACCESS COMMUNICATIONS**

Multiple access OFDM or OFDMA has recently been proposed in a number of standards and proprietary waveforms (e.g., [3]). In OFDMA, a subset of the subcarriers is allocated to each user node in a network. The users' signals must be synchronized at the receiver input to prevent ICI. OFDMA works well in the network downlink of a base station since all of the subcarriers are transmitted from the base station and can be easily synchronized. Thus, the advantages of OFDM that were mentioned above, in the section "Single-User Communications," are also applicable to OFDMA in the downlink of a network. Similarly, the advantages of FBMC that were mentioned are applicable too.

However, the situation is very different in the uplink of an OFDMA network. In particular, synchronization is no longer a trivial task. The subcarrier signals transmitted from all the (mobile) nodes should arrive at the base station synchronously, both in terms of symbol timings and carrier frequencies. Because of the presence of CP, OFDMA can tolerate some error in the timing phase. However, a close-to-perfect carrier synchronization is necessary for an acceptable operation of an OFDMA network; carrier frequencies of different users should match one another within an accuracy of 1–2% of subcarrier spacing. Although such a resolution may be possible in a stationary (i.e., nonmobile) network, the task of carrier synchronization in a network of mobile nodes becomes a very difficult task, if not impossible. Hence, in practice, it is often assumed that perfect synchronization is not achieved, and thus, addition-

al signal processing steps are added to minimize interference among signals from different nodes. Such steps add significant complexity to an OFDMA receiver.

Morelli et al. [4] have recently presented an excellent review of the OFDMA synchronization methods that have been reported in the literature. The many hard-to-handle problems that an OFDMA will face in the uplink of a network are discussed in detail. Both problems of carrier and timing synchronization have been reviewed, and it has been noted that, probably, the best method of resolving the synchronization issues is through the use of a bank of filters that separate different users; see the conclusion section of [4] for a quick note. This will clearly add additional complexity to the receiver and will require relatively wide guard bands between different user bands, and hence, will incur significant bandwidth loss. It has also been noted that the problem can be resolved by using sophisticated multiple access interference (MAI) cancellation methods. However, it was noted that such methods may be too complex to implement.

On the other hand, because of the use of near-perfect subcarrier filters, FBMC avoids MAI without any need to perform synchronization. No additional filtering is required, thanks to perfectly frequency-localized subcarriers in FBMC. Hence, a fair comparison between OFDM and FBMC, in the uplink of a multiple access network, can be made only when OFDMA adopts a MAI-cancellation method. Such a comparison has recently been reported in [72], where the following observations have been made. MAI cancellation-enabled OFDMA systems are generally over an order of magnitude more complex than their FBMC counterparts. Moreover, despite their much higher complexity, such OFDMA systems are not able to perfectly remove MAI, while FBMC suppresses MAI almost perfectly.

### **COGNITIVE RADIO COMMUNICATIONS**

The filtering property of FBMC will become more instrumental in cognitive radios where primary (noncognitive nodes) and secondary (cognitive nodes) users independently transmit and may be based on different standards. In such a setting, the only practical method that can be used for separating primary and secondary users is through filtering. (We may note that, theoretically, it is possible to use a set of independent radios to detect the primary user signals. The primary user signals are thus subtracted from the received signal, and the result will then be processed to extract the secondary user data. Clearly, this is also a filtering process.)

As discussed in the section "Filtered OFDM," filtering in OFDM has some serious limitations. In particular, when the roll-off periods  $T_0$  and  $T_1$  in the filtered OFDM are kept small to avoid a significant loss of bandwidth efficiency, the subcarrier synthesis and analysis filters, respectively, suffer from significantly wide transition bands. As a result, to keep signals from different radios (being primary or secondary) separated, a significant guard band should be introduced between the bands that belong to different users. This, clearly, corresponds to a different form of bandwidth loss. As an example, the magnitude responses



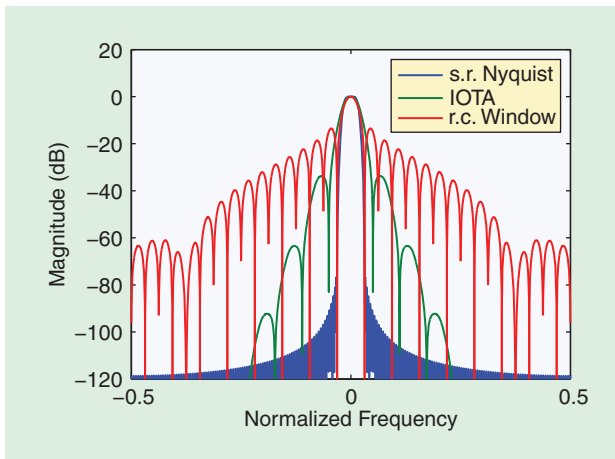


**[FIG14]** The magnitude responses of a square-root Nyquist filter, an IOTA filter, and a raised-cosine window associated with a filtered-OFDM system. The square-root Nyquist filter has been designed for an excess bandwidth 100% ( $\alpha = 1$ ). For the raised-cosine window,  $T_0 = 0.15T_{\text{FFT}}$ . Both the square-root Nyquist and IOTA filters have a length of 67 (recall that in these cases  $T = T_{\text{FFT}}$ ).

of a square-root Nyquist filter, an IOTA filter, and a raised-cosine window associated with a filtered-OFDM system are presented in Figure 14. The responses clearly show the undesirably large magnitudes of many side lobes in the case of the raised-cosine window. The square-root Nyquist filter has the best magnitude response with the smallest side lobes. This is at a cost of poor side lobes in its time-domain response, i.e., a smaller  $\sigma_f$  at the cost of a large  $\sigma_t$ ; see the section “Filter Design Methods (Advanced Designs)” for the definitions of  $\sigma_f$  and  $\sigma_t$  and the related discussions. IOTA design provides a compromised design that balances between  $\sigma_f$  and  $\sigma_t$ .

### DOUBLY DISPERSIVE CHANNELS

In the section “Filter Design Methods (Advanced Designs),” the IOTA design was proposed as an effective means for dealing with doubly dispersive channels. As it was noted, one should choose a prototype filter that strikes a balance between the channel response spreading in time (caused by multipaths) and frequency (caused by Doppler shifts in different multipaths), and IOTA design has been proposed as an effective method of striking this balance optimally. This, as was discussed, is done by minimizing the time-frequency spreading parameter  $\sigma_f\sigma_t$ . On the contrary, it is known that, in OFDM with a rectangular window,  $\sigma_f\sigma_t$  has an unbounded value. More accurately, for a fixed carrier spacing, as the number of subcarriers in OFDM increases unboundedly,  $\sigma_f\sigma_t$  approaches infinity. Accordingly, OFDM is a poor choice for doubly spread channels. In fact, many researchers have studied the issues related to doubly spread channels and concluded that FBMC methods are far better choices when compared to OFDM [52]–[55].

To quantify this observation, following the method of [54], we have recently developed a prototype filter design scheme [73] in which the symbol density  $D = 1/TF$  can be selected arbitrarily, thus allowing a straightforward comparison of OFDMA and

FBMC in doubly dispersive channels. Here, since  $D$  may be greater than 0.5, we consider an FMT-like setup where conventional QAM symbols are transmitted. This is an interesting setup as it also allows a straightforward adoption to MIMO channels. The mobility is measured by the product  $\Delta\tau\Delta\nu$ , where, as defined before,  $\Delta\tau$  and  $\Delta\nu$  are the channel spreading in time and frequency, respectively. Although the comparisons are made over a wide range of  $\Delta\tau\Delta\nu$ , the prototype filter is designed for a target value  $\Delta\tau\Delta\nu = 0.04$ . The channel multipath power profile is assumed flat over the range of  $\Delta\tau$ . This may be thought of as a worse-case scenario (for a given  $\Delta\tau$ ), as in most channels, the delay power profile is an exponentially decaying function of the location of multipaths and, hence, results in a smaller effective spreading. The channel spreading in the frequency domain is assumed to follow a Jake’s model with a maximum Doppler spread  $f_d = \Delta\nu/2$ . We note that adding the channel effect into the transmission path will result in a distorted ambiguity function, and this in turn, results in ISI and ICI; see, e.g., [20], [56], and [73] for details. The introduced ISI and ICI are evaluated for different choices of  $D$  and  $\Delta\tau\Delta\nu$ , and accordingly, the signal-to-interference power ratio (SIR) values of the detected symbols at the receiver outputs are evaluated. The result of this study is presented in Figure 15. This clearly shows the significant performance improvement of FBMC over OFDM as the channel mobility increases.

### DSL AND PLC

Communications over DSLs and power lines face a common problem, in some ways similar to those encountered in cognitive radios. These systems transmit broadband signals over unshielded wires. These broadband signals that span from low frequencies up to a few tens of megahertz are subject to interference from narrow-band long and medium wavelength AM radios as well as signals from amateur radios [22], [23], [48]. Hence, the DSL and PLC signals should be synthesized/analyzed to avoid and also not to interfere with these radio signals. As one would expect, a multicarrier modulation scheme in which the subcarriers within the bands that may contain interfering signals are nulled trivially satisfies the needs of such systems if the spectrum of each subcarrier is contained within a narrow band. From the observations made in the previous sections, it is obvious that FBMC serves this goal much better than the OFDM/filtered OFDM.

### ACTIVITIES IN THE STANDARD COMMITTEES

It appears that the earliest proposal to use FBMC for multicarrier communications is a contribution from Tzannes et al. of AWARE Inc., in one of the asymmetric DSL (ADSL) standard meeting in 1993 [31]. The proposed method that was called DWMT was further studied in [40]. Additional works on the subject were presented in many conference papers in the mid- and late-1990s; see [32] for a review of these works. Despite enthusiasm from the research community, DWMT was not adopted in the ADSL standard, partly because of the perceived complexity of this method, especially when compared with its rival, the

DMT, the name used for OFDM when applied in DSL technologies. Indeed, the DWMT structure proposed by Tzannes et al. was significantly more complex than the DMTs. The major part of the complexity of DWMT came from the equalization method that was adopted. The detailed discussion presented in [40] assumed that one needs an equalizer that combines signals from each subcarrier band and its adjacent bands to combat ISI and ICI. Typical equalizer lengths suggested in [40] were 21 real-valued taps per subcarrier. A thorough analysis of the equalization structure proposed in [40] was later presented in [41]. This study that initially reduced the complexity of the DWMT equalizer to about one third of its original form [40] was later led to a receiver structure that required only two real-valued taps for equalization of each subcarrier, [32]. Moreover, the studies in [32] (and by others, e.g., [33]) revealed that DWMT is nothing but what, in this article, we called CMT, i.e., DWMT, in effect, is a reinvention of Chang's method.

In the area of PLC, significant attempts have been made to introduce FBMC. These efforts have resulted in the inclusion of CMT in the IEEE P1901 [50], the standard that is being developed for PLC systems. In the P1901 documents, CMT/DWMT is called wavelet OFDM.

In 1999, an FBMC method with nonoverlapping subcarrier bands, like those discussed in the section "FBMC Systems for QAM Symbol Transmission," was proposed as a solution for filtering the narrow-band interferences in VDSL channels [43]. The proposed method was called FMT. This proposal that was included as an annex in one of the initial draft documents of VDSL [46] was further developed by a number of researchers [44], [45] and some have recently proposed it for wireless communication channels with high mobility, where OFDM may degrade significantly, e.g., [47]. We note that, to avoid incompatibility with ADSL, FMT was not included in the final document of the VDSL standard [59].

For the IEEE 802.22, a recent cognitive radio standard to access TV bands in wireless rural area networks (WRAN), France Telecom presented a proposal based on the SMT modulation [51]. This proposal was based on the principle described in [52]. However, this was not retained for IEEE 802.22. Up to now, the only standard for radio transmission that uses FBMC is the TIA's Digital Radio Technical Standards [58], where SMT has been adopted.

## ADDITIONAL NOTES

To present the basic ideas behind OFDM and FBMC methods and to highlight their main features without getting too far into the details, many developments in the literature were not discussed in the previous sections. This section provides an overview of these additional developments. The literature on FBMC methods, in particular, although not as extensive as that of OFDM, is somewhat broad and has been presented by researchers with different backgrounds and with a variety of different terminologies. So, in many cases, fundamentally similar works have been presented independently by different communities of researchers. This section seeks to link these works. It should be

noted that the presentation in this section is not meant to be a comprehensive review of the literature. The goal is to provide the reader with a few pointers to the more significant developments in the literature and also to list a broad range of terminologies that have been used by different researchers while referring to similar concepts.

In this article, we discussed in detail the pioneering works of Chang and Saltzberg and showed their relationship in terms of the time–frequency phase-space lattices. More details can be found in [30]. Both Chang's and Saltzberg's formulations were in terms of continuous-time synthesis and analysis filter banks. The initial idea to implement these filter banks in discrete time is due to Bellanger and Daguet [11]. More extensive work was later done by Hirosaki [12], who discussed in detail the poly-phase structures for both transmitter and receiver and also proposed methods for channel equalization. More efficient implementations were later introduced in [16] and [17]. Most of these studies have made specific reference to the Saltzberg's DSB modulation [9] under the name OFDM-OQAM.

Chang's work [8], on the other hand, has received less attention. Those who have cited [8] have only acknowledged its existence without presenting much detail, e.g., [12], [15], and [17]. For instance, Hirosaki, who has extensively studied and developed digital structures for implementation of Saltzberg's method [12], [15], has only made a brief reference to Chang's method and noted that, since it uses VSB modulation and thus its implementation require a Hilbert transformation, it is more complex than that of Saltzberg's method. He thus proceeds with a detailed discussion and development of multirate structures for the Saltzberg's method only. On the other hand, a vast amount of literature in digital signal processing has studied a class of multicarrier systems that has been referred to as DWMT. This method was discussed in the section "Activities in the Standard Committees."

It is also interesting to note that the researchers who studied digital filter banks developed a class of filter banks that were called modified DFT (MDFT) filter bank [34]. Careful study of MDFT reveals that this, although developed independently, is

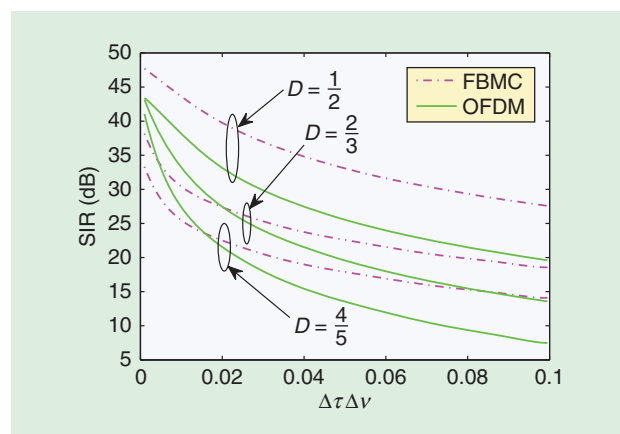


**[FIG15]** Performance comparison of OFDM and CMFB in channels with mobilities.

essentially a reformulation of Saltzberg's filter bank in discrete time and with emphasis on compression/coding. The literature on MDFT begins with the pioneering works of Fliege [35] and has been extended by others later, e.g., [36]–[39].

The first comprehensive study and adaptation of FBMC to match the channel time and frequency dispersions was presented in [52]. We summarized the most significant results of [52] in the section “Filter Design Methods (Advanced Designs)”; the introduction of the IOTA filter design. This elegant design, that had been invented earlier by Alard [53], begins with a Gaussian pulse and through a couple of orthogonalization steps (32) obtains a prototype filter that satisfies the orthogonality condition (20). The IOTA design was further studied in [19], where the authors proposed a closed-form equation (in terms of Fourier series) for the impulse response of the class of IOTA filters. These were called extended Gaussian functions (EGFs). The most pertinent advantage of IOTA design is its optimum time–frequency localization, in the sense that it minimizes the time–frequency localization product  $\sigma_t \sigma_f$ , where the parameters  $\sigma_t$  and  $\sigma_f$  are defined according to (25) and (26), respectively. This localization property of IOTA design is formally proved in [55]. Another class of functions that offers a similar time–frequency localization were proposed in [54]. These designs are called Hermite filters. It was noted that the set of functions  $D_n(t) = h_n(\sqrt{2\pi}t)$ , for  $n = 0, 4, 8, \dots$ , where  $h_n(t) = e^{-t^2/2}(d^n/dt^n)e^{-t^2}$ , satisfy the identity  $\mathcal{F}D_n(t) = D_n(f)$ . It was thus concluded that a pulse shape  $p(t)$  formed by linearly combining  $D_n(t)$ , for

$n = 0, 4, 8, \dots$  also satisfies the identity  $\mathcal{F}p(t) = p(f)$ . Hence, a procedure for combining  $D_n(t)$  functions to construct a pulse shape  $p(t)$  whose ambiguity function satisfies the orthogonality condition (20) was proposed. A more recent development is [73], where the authors followed the Hermite design, but set their design goal to widen the nulls in the ambiguity function  $A_p(\tau, \nu)$ , thus, lead to a design that is robust to doubly dispersive channel effects. The results that were presented in Figure 15 are based on this design.

Both IOTA and Hermite designs assume that the same prototype filter is used for signal synthesis at the transmitter and signal analysis at the receiver. In [20] and [65], the authors noted that the use of similar prototype filters at the transmitter and receiver is suboptimal and, for a given set of channel parameters, proposed a design method for selection of a pair of optimum biorthogonal prototype filters. Some researchers have used the terminology OFDM with pulse shaping when reference is made to SMT/OFDM-OQAM, e.g., [13], [65].

The time–frequency phase-space lattice structures presented in Figures 3, 7, and 12 have a square/rectangular structure. Using results from sphere packing theory, it has been noted that more robust transmission can be achieved by arranging the lattice points in a hexagonal structure, e.g., see [55] and [56]. This arrangement is visualized in Figure 16, where one finds that, for the same density of the points, the hexagonal lattice leads to a wider distance between the points. The most recent advancement in the area of improving the spectral efficiency of FBMC is [57], where the authors have proposed a method for using a lattice with a density  $1/(TF) > 1$ . The designs whose results were presented in Figure 15, to compare FBMC and OFDM in mobile channels, are based on a hexagonal time–frequency phase-space lattice.

## CONCLUSIONS

This article set the goal of identifying the pros and cons of OFDM when compared with the class of multicarrier techniques that use filter banks for signal synthesis and analysis, namely, FBMC. It was noted that, while OFDM offers a lower complexity and is more robust to timing offset, FBMC offers a number of other advantages that may make it a more viable technology for many upcoming and future communication systems. FBMC systems outperform OFDM in the following areas:

- In the uplink of an OFDMA network, an almost perfect carrier synchronization of signals from different transmitting nodes is necessary. In practice, particularly in mobile networks, this is a very hard task to achieve. FBMC systems achieve signal separation through filtering, thus avoiding the need for (close to) perfect carrier synchronization. Separation of the different users' signals through a filtering process also avoids the need for any timing synchronization between the users. While the detailed presentation in the section “Filtered OFDM” showed significant limitations of OFDM in separating different user signals through a filtering process, the discussion in the rest of

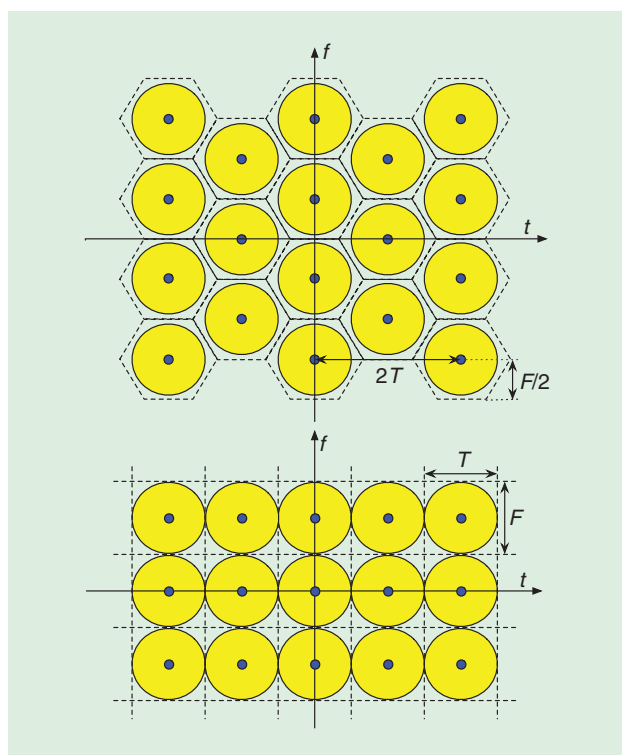


**[FIG16]** Comparison of rectangular and hexagonal time–frequency phase-space lattices. The yellow circles in both cases have the same radius.

the article did emphasize the fact that FBMC is a design that features a near-ideal filtering property that is innate to its formulation.

- In cognitive radios, the filtering capability of FBMC systems makes them the perfect choice for filling in the spectrum holes.

- OFDM is known to be sensitive to fast variations of the communication channels. FBMC systems, on the other hand, can be designed to be equally robust to channel time and frequency spreading. Such designs are based on IOTA prototype filters that were discussed in the section “Filter Design Methods (Advanced Designs).”

- The well-designed prototype filters in FBMC make this modulation a perfect match to the applications such as PLC and DSL communication systems, where the channel is subject to a number of high-power interfering narrow-band signals.

On the other hand, we noted that OFDM has a number of desirable features, including low complexity of implementation and mature technologies that keep it the dominant technology for single-user (point-to-point) communications. Moreover, while OFDM can be easily adopted for MIMO channels, development of MIMO-FBMC systems/networks is nontrivial and may be very limited. Only FMT, the less bandwidth-efficient member of the class of FBMC systems, can offer a similar level of flexibility as OFDM in MIMO channels.

To summarize, the poor frequency spectra of subcarrier signals in OFDM is the main source of problems that limit the applicability of OFDM in some present and future development of broadband communication systems. FBMC, on the other hand, is an elegant method that resolves most of these problems by taking a filtering approach to multicarrier communications. It is, thus, the view of the author of this article that as the shortcomings of OFDM/OFDMA prevails in the present and future applications, FBMC will eventually arise as an effective replacement. With this potential in sight, it is this author's hope that the material presented in this article will stimulate more research in the area of FBMC.

## SUGGESTIONS FOR FURTHER RESEARCH

Unlike OFDM, whose performance has been studied from virtually any point of view, most studies related to FBMC have remained in the realm of theoretical developments. In particular, most studies assume perfect timing and carrier synchronization at the receiver. Although limited studies have been reported in the areas related to synchronization of FBMC receivers, e.g., [64]–[68], more thorough studies are necessary for the FBMC to mature. From the discussion in this article, it may be evident that in the areas of the uplink of a multiple access network and cognitive radios FBMC is superior to OFDM/OFDMA. More research for quantifying this fact is a great need. Another area where there is a need for further study is application of FBMC systems to MIMO channels. The use of real/PAM symbols in SMT and CMT makes their extension to MIMO systems nontrivial. Some limited studies to apply SMT and/or CMT to MIMO systems have been reported

in [70] and [71]; however, these are only for very specific applications. Moreover, as noted above, FMT can be trivially applied to MIMO channels similar to OFDM. However, FMT has lower bandwidth efficiency than SMT and CMT. Nevertheless, FMT systems with a similar bandwidth efficiency to that of OFDM is possible. Thus, for MIMO channels, FMT-based FBMC is a good compromised choice to study.

## ACKNOWLEDGMENTS

This work has been supported by the National Science Foundation under award 0801641.

## AUTHOR

**Behrouz Farhang-Boroujeny** (farhang@ece.utah.edu) received his B.Sc. degree in electrical engineering from Teheran University, Iran, in 1976, his M.Eng. degree from the University of Wales Institute of Science and Technology, United Kingdom, in 1977, and his Ph.D. degree from Imperial College, University of London, United Kingdom, in 1981. He is an expert in the general area of signal processing. In the past, he has worked and has made significant contribution to areas of adaptive filters theory, acoustic echo cancellation, magnetic/optical recoding, statistical MIMO detection methods, and cognitive radios. He is currently a professor in the Electrical and Computer Engineering Department at the University of Utah. He is the author of the books *Adaptive Filters: Theory and Applications* (Wiley, 1998) and *Signal Processing Techniques for Software Radios* [Lulu Publishing House, 2008 (first edition) and 2010 (second edition)]. He is a Senior Member of the IEEE. His current scientific interests are adaptive filters, multicarrier communications, detection techniques for space-time coded systems, and cognitive radios.

## REFERENCES

- [1] R. Van Nee and R. Prasad, *OFDM for Wireless Multimedia Communications*. Boston, MA: Artech House, 2000.
- [2] Y. Li and G. L. Stüber, Eds., *Orthogonal Frequency Division Multiplexing for Wireless Communications*. New York, NY: Springer-Verlag, 2006.
- [3] *Air Interface for Fixed and Mobile Broadband Wireless Access Systems*, IEEE Standard 802.16e, 2005.
- [4] M. Morelli, C.-C. Jay Kuo, and M.-O. Pun, “Synchronization techniques for orthogonal frequency division multiple access (OFDMA): A tutorial review,” *Proc. IEEE*, vol. 95, no. 7, pp. 1394–1427, July 2007.
- [5] T. A. Weiss and F. K. Jondral, “Spectrum pooling: An innovative strategy for the enhancement of spectrum efficiency,” *IEEE Commun. Mag.*, vol. 42, no. 3, pp. S8–S14, Mar. 2004.
- [6] S. Pagadarai, R. Rajbanshi, A. M. Wyglinski, and G. J. Minden, “Sidelobe suppression for OFDM-based cognitive radios using constellation expansion,” in *Proc. IEEE Wireless Communications and Networking Conf.*, Mar. 31–Apr. 3, 2008, pp. 888–893.
- [7] B. Farhang-Boroujeny and R. Kemper, “Multicarrier communication techniques for spectrum sensing and communication in cognitive radios,” *IEEE Commun. Mag. (Special Issue on Cognitive Radios for Dynamic Spectrum Access)*, vol. 46, no. 4, pp. 80–85, Apr. 2008.
- [8] R. W. Chang, “High-speed multichannel data transmission with bandlimited orthogonal signals,” *Bell Syst. Tech. J.*, vol. 45, pp. 1775–1796, Dec. 1966.
- [9] B. R. Saltzberg, “Performance of an efficient parallel data transmission system,” *IEEE Trans. Commun. Tech.*, vol. 15, no. 6, pp. 805–811, Dec. 1967.
- [10] S. Weinstein and P. Ebert, “Data transmission by frequency-division multiplexing using the discrete Fourier transform,” *IEEE Trans. Commun. Tech.*, vol. 19, no. 5, part 1, pp. 628–634, Oct. 1971.
- [11] M. Bellanger and J. Daguet, “TDM-FDM transmultiplexer: Digital polyphase and FFT,” *IEEE Trans. Commun.*, vol. 22, no. 9, pp. 1199–1205, Sept. 1974.
- [12] B. Hirosaki, “An orthogonally multiplexed QAM system using the discrete Fourier transform,” *IEEE Trans. Commun.*, vol. 29, no. 7, pp. 982–989, July 1981.



- [13] H. Bölcskei, P. Duhamel, and R. Hleiss, "Orthogonalization of OFDM-OQAM pulse shaping filters using the discrete Zak transform," *Signal Processing*, vol. 83, no. 7, pp. 1379–1391, July 2003.
- [14] H. Bölcskei, "Orthogonal frequency division multiplexing based on offset QAM," in *Advances in Gabor Analysis*, H. G. Feichtinger and T. Strohmer, Eds. Cambridge, MA: Birkhäuser, pp. 321–352, 2003.
- [15] B. Hirotsaki, S. Hasegawa, and A. Sabato "Advanced groupband data modem using orthogonally multiplexed QAM technique," *IEEE Trans. Commun.*, vol. 34, no. 6, pp. 587–592, June 1986.
- [16] G. Cariolaro and F. C. Vaglini, "An OFDM scheme with a half complexity," *IEEE J. Select. Areas Commun.*, vol. 13, no. 9, pp. 1586–1599, Dec. 1995.
- [17] L. Vangelista and N. Laurenti, "Efficient implementations and alternative architectures for OFDM-OQAM systems," *IEEE Trans. Commun.*, vol. 49, no. 4, pp. 664–675, Apr. 2001.
- [18] P. Siohan, C. Siclet, and N. Lacaille, "Analysis and design of OFDM-OQAM systems based on filterbank theory," *IEEE Trans. Signal Processing*, vol. 50, no. 5, pp. 1170–1183, May 2002.
- [19] P. Siohan and C. Roche, "Cosine-modulated filterbanks based on extended Gaussian functions," *IEEE Trans. Signal Processing*, vol. 48, no. 11, pp. 3052–3061, Nov. 2000.
- [20] W. Kozek and A. F. Molisch, "Nonorthogonal pulseshapes for multicarrier communications in doubly dispersive channels," *IEEE J. Select. Areas Commun.*, vol. 16, no. 8, pp. 1579–1589, Oct. 1998.
- [21] G. W. Wornell, "Emerging applications of multirate signal processing and wavelets in digital communications," *Proc. IEEE*, vol. 84, no. 4, pp. 586–603, Apr. 1996.
- [22] W. Y. Chen, *DSL Simulation Techniques and Standards Development for Digital Subscriber Line Systems*. Indianapolis, IN: Macmillan, 1998.
- [23] T. Starr, J. M. Cioffi, and P. J. Silverman, *Understanding Digital Subscriber Line Technology*. Upper Saddle River, NJ: Prentice-Hall, 1999.
- [24] F. Sjöberg, M. Isaksson, R. Nilsson, P. Odling, S. K. Wilson, and P. O. Borjesson, "Zipper: A duplex method for VDSL based on DMT," *IEEE Trans. Commun.*, vol. 47, no. 8, pp. 1245–1252, Aug. 1999.
- [25] D. G. Mestdagh, M. R. Isaksson, and P. Odling, "Zipper VDSL: A solution for robust duplex communication over telephone lines," *IEEE Commun. Mag.*, vol. 38, no. 5, pp. 90–96, May 2000.
- [26] A. Skrzypczak, P. Siohan, and J.-P. Javaudin, "Application of the OFDM/OQAM modulation to power line communications," in *Proc. IEEE Int. Symp. Power Line Communications and Its Applications (ISPLC '07)*, Pisa, Italy, Mar. 26–28, 2007, pp. 71–76.
- [27] K. H. Afkhamie, S. Kata, L. Yonge, and R. Newman, "An overview of the upcoming HomePlug AV standard," in *Proc. Int. Symp. Power Line Communications and Its Applications*, 2005, pp. 400–404.
- [28] B. Farhang-Boroujeny, "A square-root Nyquist (M) filter design for digital communication systems," *IEEE Trans. Signal Processing*, vol. 56, no. 5, pp. 2127–2132, May 2008.
- [29] R. D. Gitlin and E. Y. Ho, "The performance of staggered quadrature amplitude modulation in the presence of phase jitter," *IEEE Trans. Commun.*, vol. 23, no. 3, pp. 348–352, Mar. 1975.
- [30] B. Farhang-Boroujeny and C. H. G. Yuen. (2010). Cosine modulated and off-set QAM filter bank multicarrier techniques: A continuous-time prospect. *EURASIP J. Adv. Signal Processing* [Online]. 2010, 16 p, DOI: 10.1155/2010/165654. Available: <http://www.hindawi.com/journals/asp/2010/165654.cta.html>
- [31] M. A. Tzannes, M. C. Tzannes, and H. Resnikoff, "The DWMT: A multicarrier transceiver for ADSL using M-band wavelet transforms," Aware, Inc., Cambridge, MA, ANSI Contribution T1E1.4/93-067, Mar. 1993.
- [32] B. Farhang-Boroujeny, "Multicarrier modulation with blind detection capability using cosine modulated filter banks," *IEEE Trans. Commun.*, vol. 51, no. 12, pp. 2057–2070, Dec. 2003.
- [33] S. Govardhanagiri, T. Karp, P. Heller, and T. Nguyen, "Performance analysis of multicarrier modulation systems using cosine modulated filter banks," in *Proc. ICASSP'99*, 1999, vol. 3, pp. 1405–1408.
- [34] N. J. Fliege, *Multirate Digital Signal Processing*. New York: Wiley, 1994.
- [35] N. J. Fliege, "Modified DFT polyphase SBC filter banks with almost perfect reconstruction," in *Proc. Int. Conf. Acoustics, Speech, and Signal Processing, ICASSP*, Apr. 1994, vol. 3, pp. III-149–III-152.
- [36] T. Karp and N. J. Fliege, "Modified DFT filter banks with perfect reconstruction," *IEEE Trans. Circuits Syst. II*, vol. 46, no. 11, pp. 1404–1414, Nov. 1999.
- [37] R. Bregovic and T. Saramaki, "A systematic technique for designing linear-phase FIR prototype filters for perfect-reconstruction cosine-modulated and modified DFT filterbanks," *IEEE Trans. Signal Processing*, vol. 53, no. 8, pp. 3193–3201, Aug. 2005.
- [38] S. Salcedo-Sanz, F. Cruz-Roldan, and X. Yao, "Evolutionary design of digital filters with application to subband coding and data transmission," *IEEE Trans. Signal Processing*, vol. 55, no. 4, pp. 1193–1203, Apr. 2007.
- [39] P. N. Heller, T. Karp, and T. Q. Nguyen, "A general formulation of modulated filter banks," *IEEE Trans. Signal Processing*, vol. 47, no. 4, pp. 986–1002, Apr. 1999.
- [40] S. D. Sandberg and M. A. Tzannes, "Overlapped discrete multitone modulation for high speed copper wire communications," *IEEE J. Select. Areas Commun.*, vol. 13, no. 9, pp. 1571–1585, Dec. 1995.
- [41] B. Farhang-Boroujeny and L. Lin, "Analysis of post-combiner equalizers in cosine modulated filter bank based transmultiplexer systems," *IEEE Trans. Signal Processing*, vol. 51, no. 12, pp. 3249–3262, Dec. 2003.
- [42] L. Lin and B. Farhang-Boroujeny, "Cosine modulated multitone for very high-speed digital subscriber lines," *EURASIP J. Appl. Signal Processing*, vol. 2006, 16 p., 2006, Article ID 19329.
- [43] G. Cherubini, E. Eleftheriou, and S. Olcer, "Filtered multitone modulation for VDSL," in *Proc. IEEE Globecom'99*, vol. 2, 1999, pp. 1139–1144.
- [44] G. Cherubini, E. Eleftheriou, S. Olcer, and J. M. Cioffi, "Filter bank modulation techniques for very high speed digital subscriber lines," *IEEE Commun. Mag.*, vol. 38, no. 5, pp. 98–104, May 2000.
- [45] G. Cherubini, E. Eleftheriou, and S. Olcer, "Filtered multitone modulation for very high-speed digital subscriber lines," *IEEE J. Select. Areas Commun.*, vol. 20, no. 5, pp. 1016–1028, June 2002.
- [46] "Very-high bit-rate digital subscriber lines (vdsl) metallic interface, part 3: Technical specification of a multi-carrier modulation transceiver," Working Group R1E1.4, Savannah, GA, Document T1E1.4/2000-013R3, Nov. 13–17, 2000.
- [47] T. Wang, J. Proakis, and J. Zeidler "Interference analysis of filtered multitone modulation over time-varying frequency-selective fading channels," *IEEE Trans. Commun.*, vol. 55, no. 4, pp. 717–727, Apr. 2007.
- [48] X. Carcellem, *Power Line Communications in Practice*. Boston: Artech House, 2006.
- [49] Available: <http://www.homeplug.org/home>
- [50] (2009). IEEE P1901 draft standard for broadband over power line networks: Medium access control and physical layer specifications [Online]. Available: <http://grouper.ieee.org/groups/1901/>
- [51] M. Bellec and P. Pirat. (2006, Jan.). OQAM performances and complexity. IEEE P802.22 Wireless Regional Area Network [Online]. Available: [http://www.ieee802.org/22/Meeting\\_documents/2006\\_Jan/index.html](http://www.ieee802.org/22/Meeting_documents/2006_Jan/index.html)
- [52] B. Le Floch, M. Alard, and C. Berrou, "Coded orthogonal frequency division multiplex," *Proc. IEEE*, vol. 83, no. 6, pp. 982–996, June 1995.
- [53] M. Alard, "Construction of a multicarrier signal," Patent WO 96/35278, 1996.
- [54] R. Haas and J.-C. Belfiore, "A time-frequency well-localized pulse for multiple carrier transmission," *Wireless Pers. Commun.*, vol. 5, pp. 1–18, 1997.
- [55] T. Strohmer and S. Beaver, "Optimal OFDM design for time-frequency dispersive channels," *IEEE Trans. Commun.*, vol. 51, no. 7, pp. 1111–1122, July 2003.
- [56] F.-M. Hand and X. D. Zhang, "Hexagonal multicarrier modulation: A robust transmission scheme for time-frequency dispersive channels," *IEEE Trans. Signal Processing*, vol. 55, no. 5, part 1, pp. 1955–1961, May 2007.
- [57] F.-M. Hand and X. D. Zhang, "Wireless multicarrier digital transmission via Weyl-Heisenberg frames over time-frequency dispersive channels," *IEEE Trans. Commun.*, vol. 57, no. 6, pp. 1721–1733, June 2009.
- [58] *Wideband Air Interface Isotropic Orthogonal Transform Algorithm-Public Safety Wideband Data Standards Project Digital Radio Technical Standards*, TIA Committee TR-8.5, 2003.
- [59] *Very High Speed Digital Subscriber Line Transceivers 2 (VDSL2)*, ITU-T Recommendation G.993.2, Feb. 2006.
- [60] F. J. Harris, "On the use of windows for harmonic analysis with the discrete Fourier transform," *Proc. IEEE*, vol. 66, no. 1, pp. 51–83, Jan. 1978.
- [61] P. P. Vaidyanathan, *Multirate Systems and Filter Banks*. Englewood Cliffs, NJ: Prentice-Hall, 1993.
- [62] J. G. Proakis, *Digital Communications*, 3rd ed. New York: McGraw-Hill, 1995.
- [63] B. Boashash, Ed., *Time Frequency Signal Analysis and Processing: A Comprehensive Reference*. Oxford, U.K.: Elsevier, 2003.
- [64] H. Bölcskei, "Blind estimation of symbol timing and carrier frequency offset in wireless OFDM systems," *IEEE Trans. Commun.*, vol. 49, no. 6, pp. 988–999, June 2001.
- [65] S. Das and P. Schniter, "Max-SINR ISI/ICI-shaping multicarrier communication over the doubly dispersive channel," *IEEE Trans. Signal Processing*, vol. 55, no. 12, pp. 5782–5795, Dec. 2007.
- [66] T. Fusco and M. Tanda, "Blind frequency-offset estimation for OFDM/OQAM systems," *IEEE Trans. Signal Processing*, vol. 55, no. 5, pp. 1828–1836, May 2007.
- [67] T. Fusco, A. Petrella, and M. Tanda, "A Data-aided symbol timing estimation for OFDM/OQAM systems," in *Proc. 2009 IEEE Int. Conf. Communications (ICC 2009)*, Dresden, Germany, June 14–18, 2009, pp. 1–5.
- [68] P. Amini and B. Farhang-Boroujeny, "Packet format design and decision directed tracking methods for filter bank multicarrier systems," *EURASIP J. Adv. Signal Processing*, vol. 2010, 13 p., 2010, DOI: 10.1155/2010/307983.
- [69] B. Farhang-Boroujeny, *Adaptive Filters: Theory and Applications*. Chichester, UK: Wiley, 1998.
- [70] B. Farhang-Boroujeny and C. Schlegel, "Efficient multicarrier realization of full-rate space-time orthogonal block coded systems," in *Proc. IEEE Int. Conf. Communications, ICC '03*, May 11–15, 2003, vol. 4, pp. 2267–2271.
- [71] C. Lélé, P. Siohan, and R. Legouable, "The Alamouti scheme with CDMA-OFDM/OQAM," *EURASIP J. Adv. Signal Processing*, vol. 2010, 13 p., 2010, DOI: 10.1155/2010/703513.
- [72] H. S. Sourck, Y. Wu, J. W. M. Bergmans, S. Sadri, and B. Farhang-Boroujeny, "Complexity and performance comparison of filter bank multicarrier and OFDM in uplink of multicarrier multiple access networks," *IEEE Trans. Signal Processing*, accepted for publication.
- [73] P. Amini, C. H. Yuen, R.-R. Chen, and B. Farhang-Boroujeny, "Isotropic filter design for MIMO filter bank multicarrier communications," in *Proc. IEEE Sensor Array and Multichannel Signal Processing Workshop (SAM)*, 2010, pp. 89–92.